FSP
Erforschung
von Universum
und Materie

Bundesministerium
für Bildung
und Forschung

ATLAS EXPERIMENT

universität freiburg

# Measurements of Higgs boson properties in decays to two $\tau$ leptons and search for lepton-flavor-violating Higgs boson decays into $\tau$ leptons using the ATLAS detector


Ö. Oğul Öncel (University of Freiburg)

on behalf of the ATLAS Collaboration


TAU2023 International Workshop
Louisville, KY, USA - 6 December 2023

# Higgs Boson Production at the Large Hadron Collider

- The center-of-mass collision energy at LHC during Run-2 (2015-2018) was $\sqrt{s}$ = 13 TeV
- Standard Model (SM) Higgs boson is produced (~ $8\times10^6$ at Run-2) via 4 major processes at the LHC

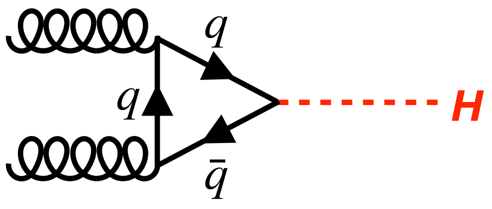


*Gluon-gluon fusion (ggF) ~ 49 pb*

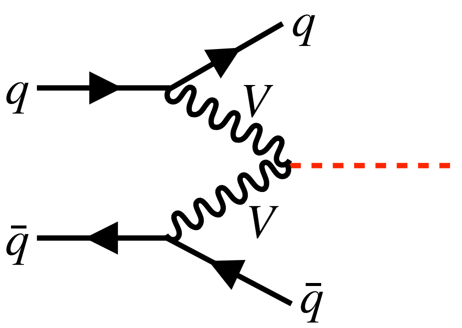


*Vector-boson fusion (VBF) ~ 4 pb*

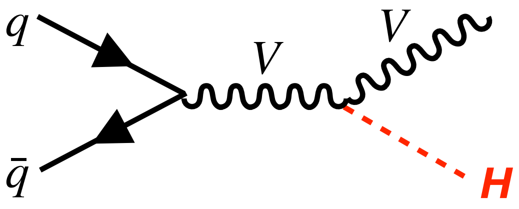


*Higgs-Strahlung (VH) ~ 2.5 pb*

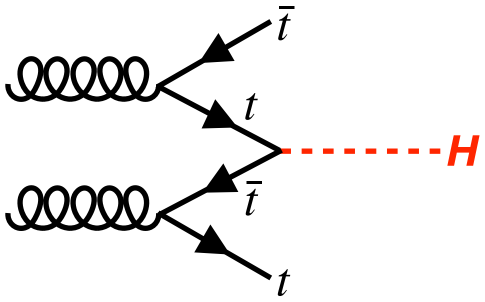


$t\bar{t}H/b\bar{b}H$ ***(HF) ~ 0.5 pb each***

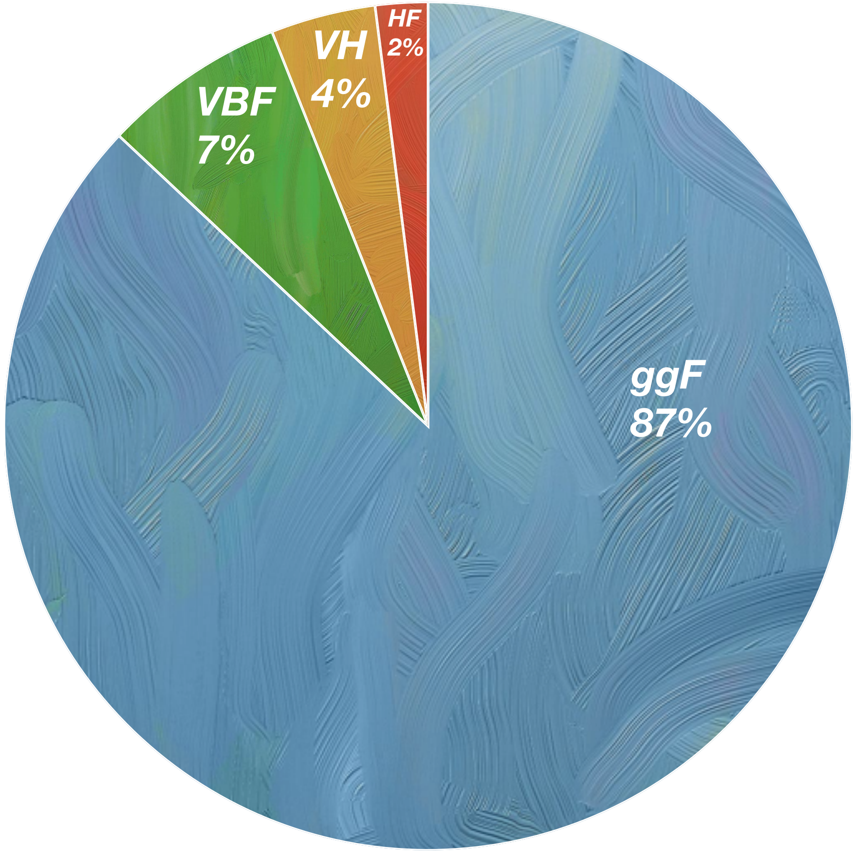

[1] Phys. Rev. D 99 (2019) 072001

- ***H*** $\rightarrow \tau\tau$ **decay channel is first observed in 2018[1] and it has the strongest Yukawa coupling ($\kappa_\tau$) to leptons**
- **It provides a compromise between a reasonable branching ratio (~6%) and signal discrimination performance**

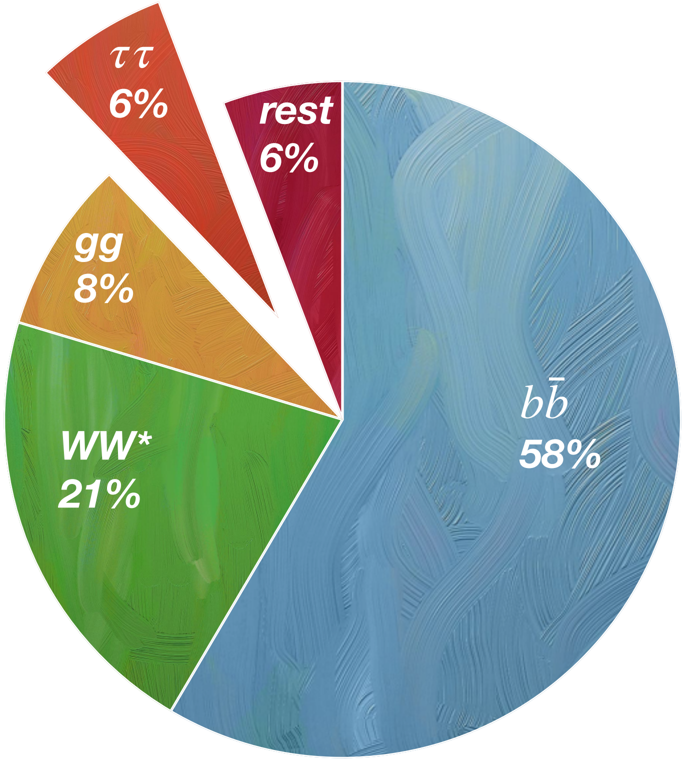


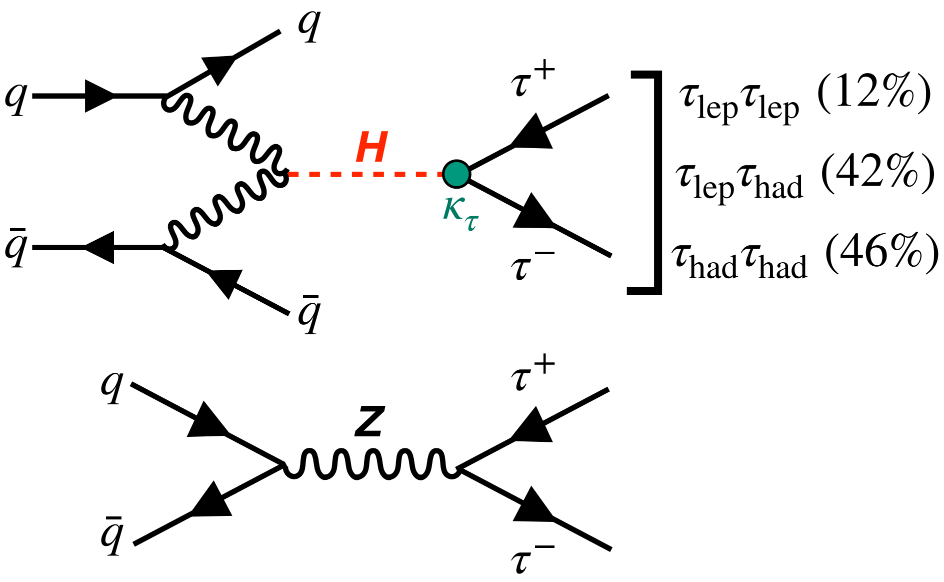


***Z*** $\rightarrow \tau\tau$ ***is the dominant background***
***(~500 times larger production rate)***

# ATLAS Experiment During Run-2: Detector and Dataset

**ATLAS is a general-purpose detector with three main components: Inner Detector, Calorimeters and Muon Chamber**

- **Algorithms combine & process information from subsystems to identify and reconstruct the particles**
- **Neutrinos escape the detector, visible transverse momentum imbalance ($E_{\mathrm{T}}^{\mathrm{miss}}$) is used as a proxy**

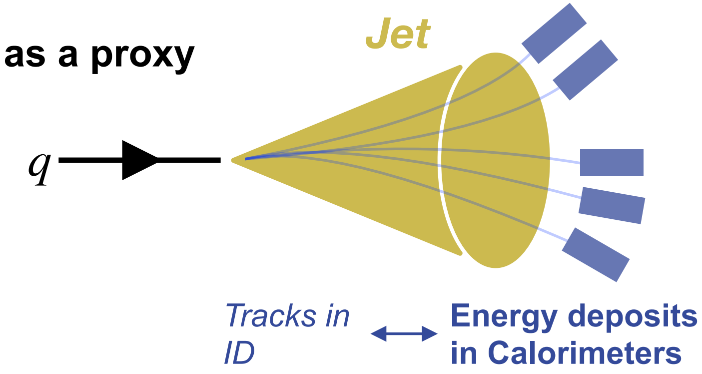


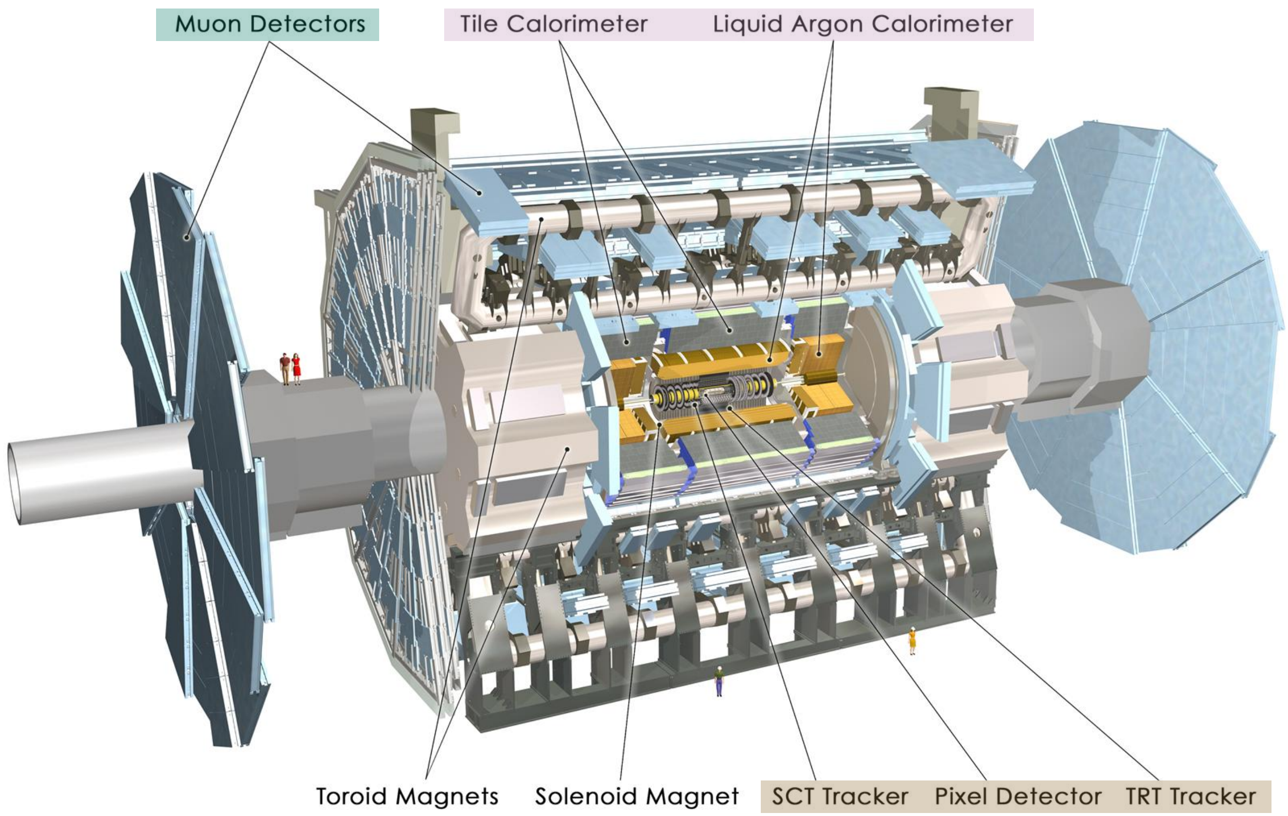


*Image Credit: ATLAS, modified*

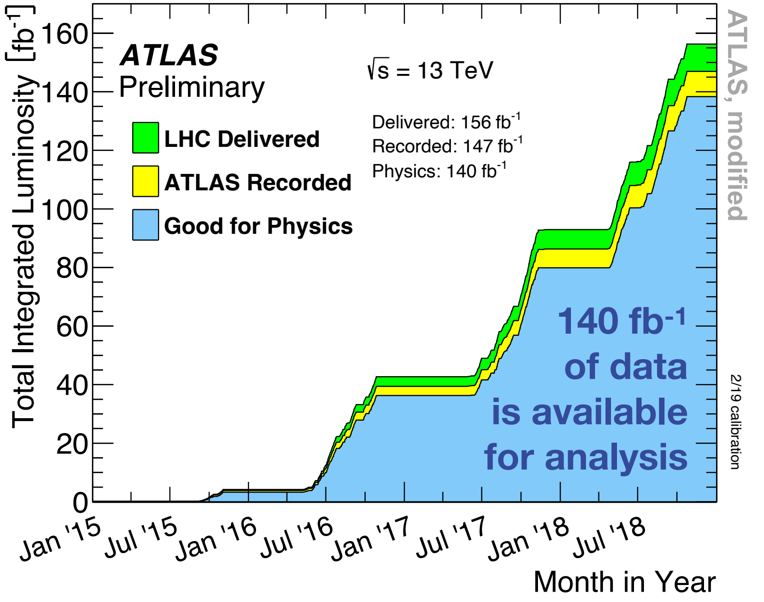

**Tau and Higgs particles decay before entering detector volume, they are reconstructed from their subsequent decay particles**

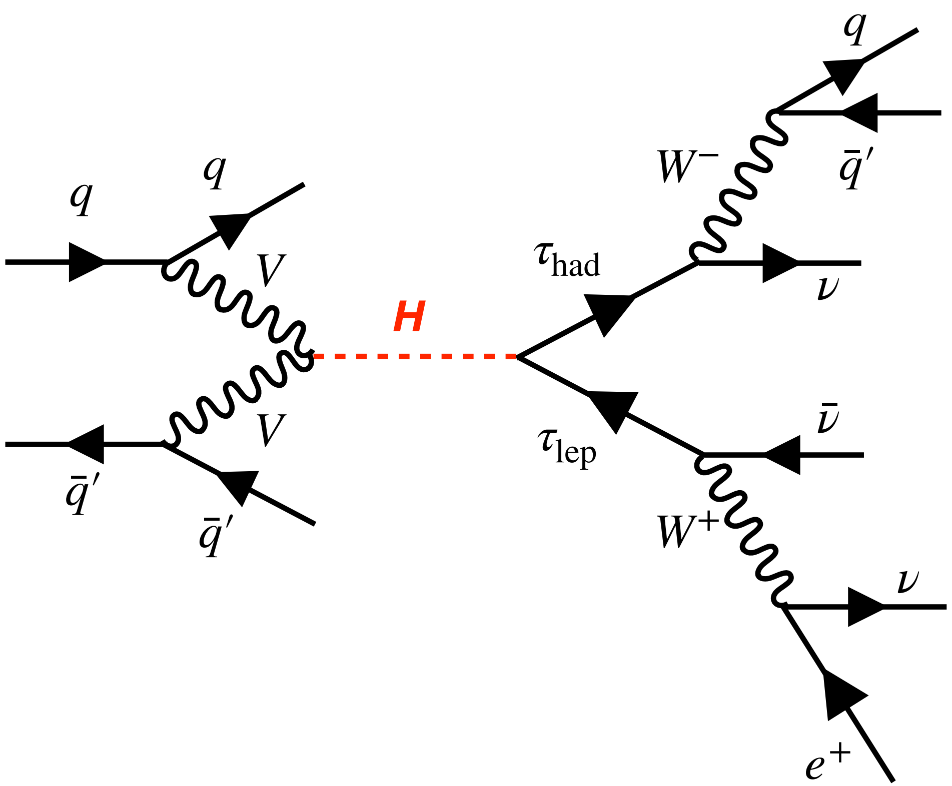

**Tau and Higgs particles decay before entering detector volume, they are reconstructed from their subsequent decay particles**

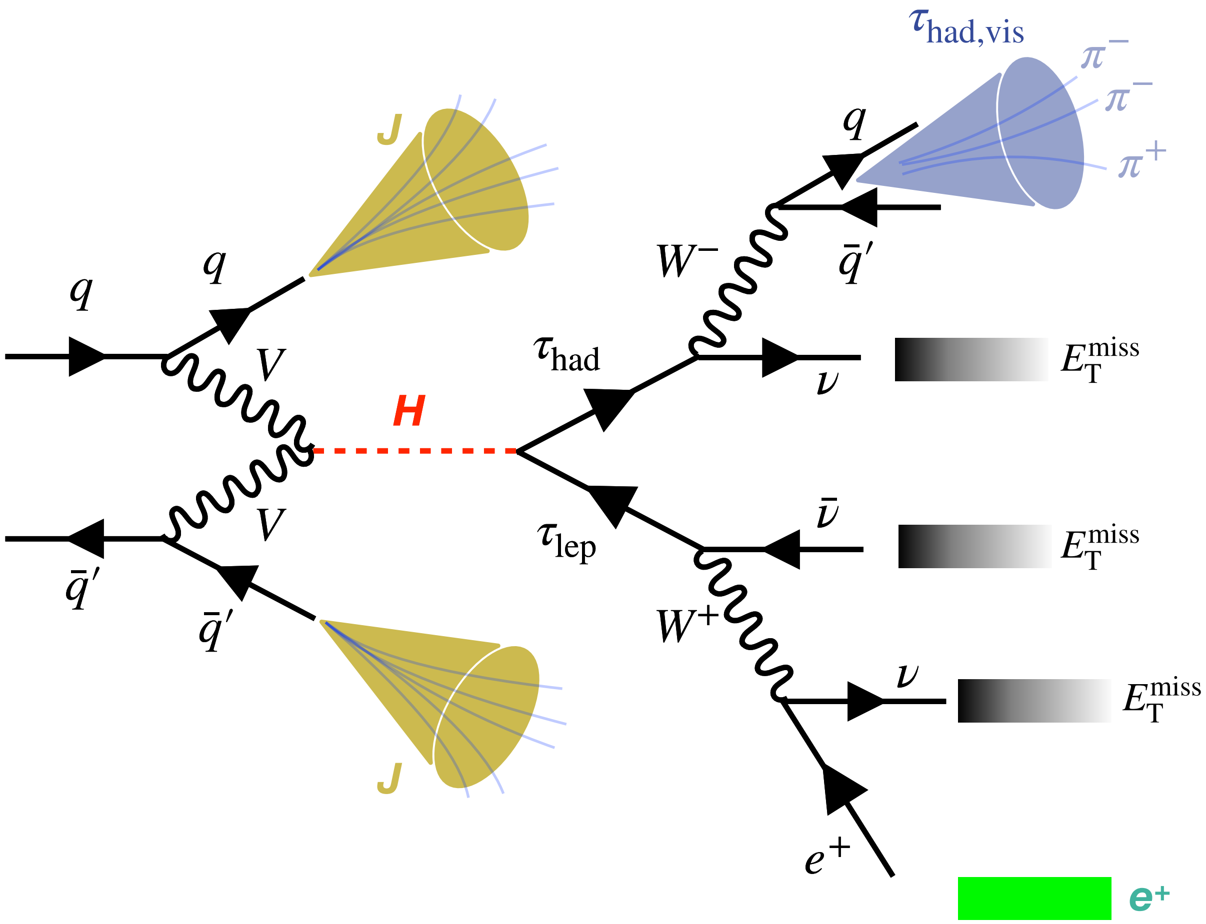

**Tau and Higgs particles decay before entering detector volume, they are reconstructed from their subsequent decay particles**

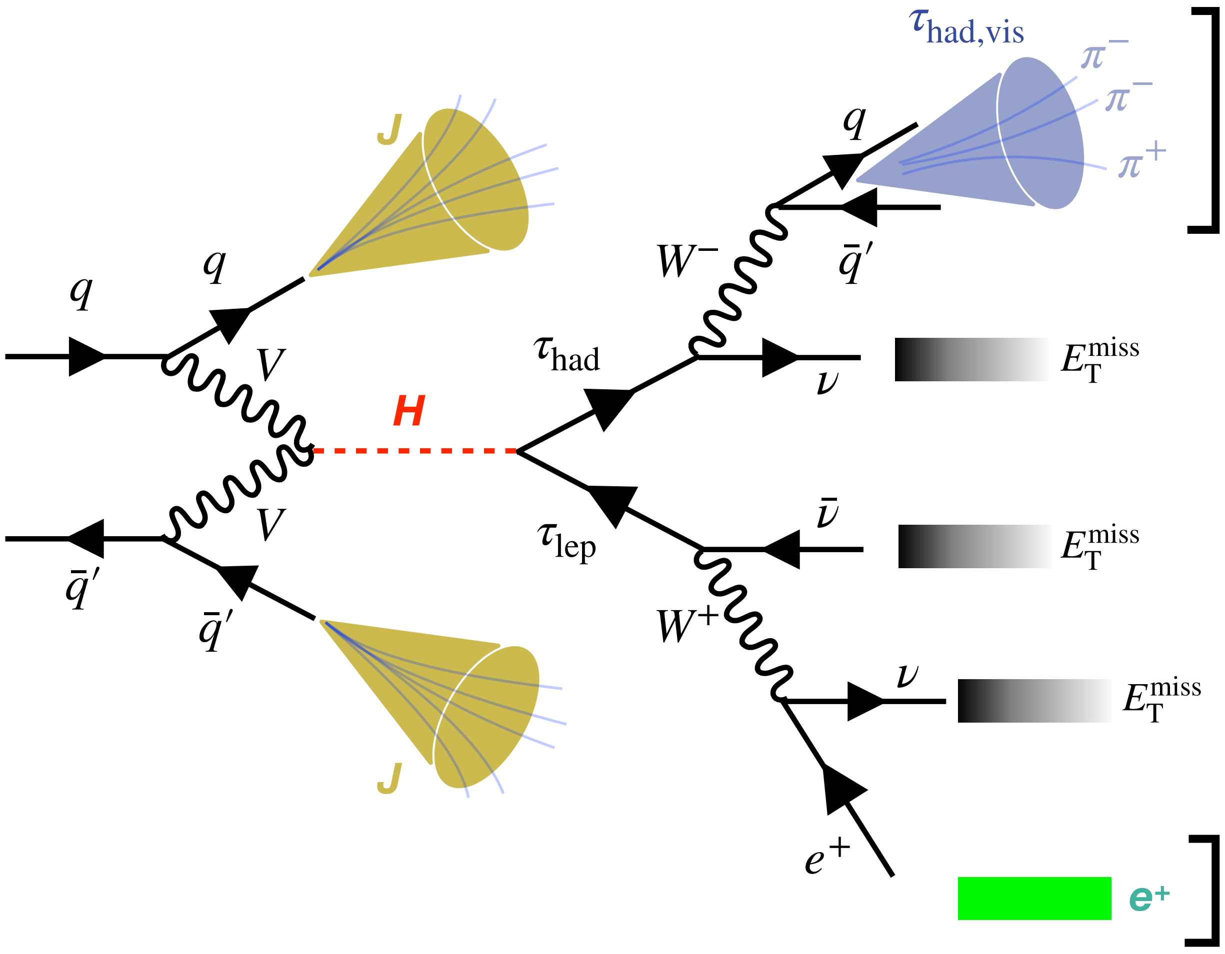


$\tau_{\text{had}} = \tau_{\text{had,vis}}$

$= \Sigma$visible decay products

**MVA discriminants against**
**$J/e \rightarrow \tau_{\text{had}}$ misidentification**
**Calibrated at Working Points**

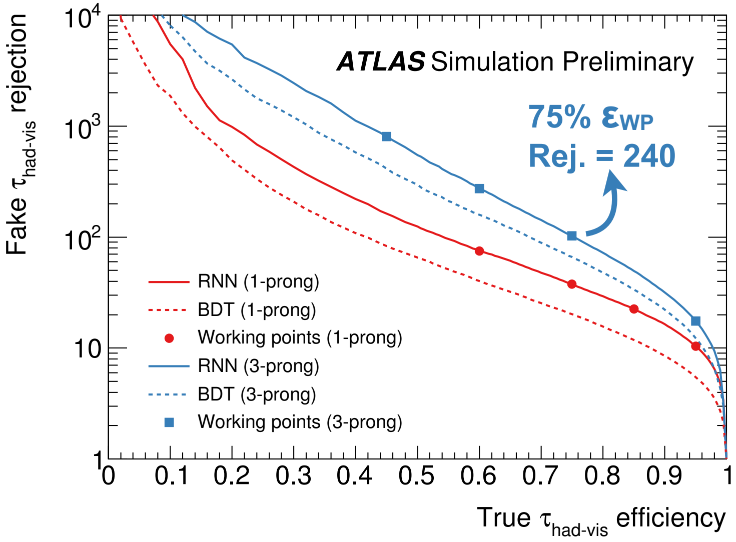


ATL-PHYS-PUB-2019-033, modified

**Likelihood-based**
**Missing Mass Calculator (MMC) algorithm[1]**

**Assumption: $E_T^{\text{miss}}$ only from *H***

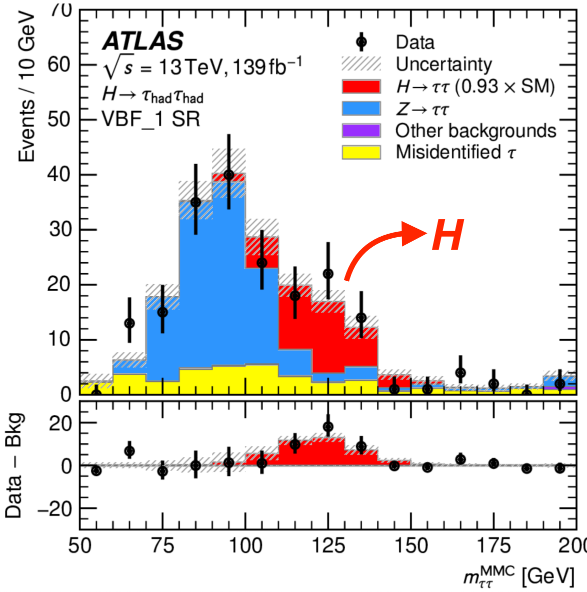


JHEP 08, 175 (2022), modified

**Tau and Higgs particles decay before entering detector volume, they are reconstructed from their subsequent decay particles**

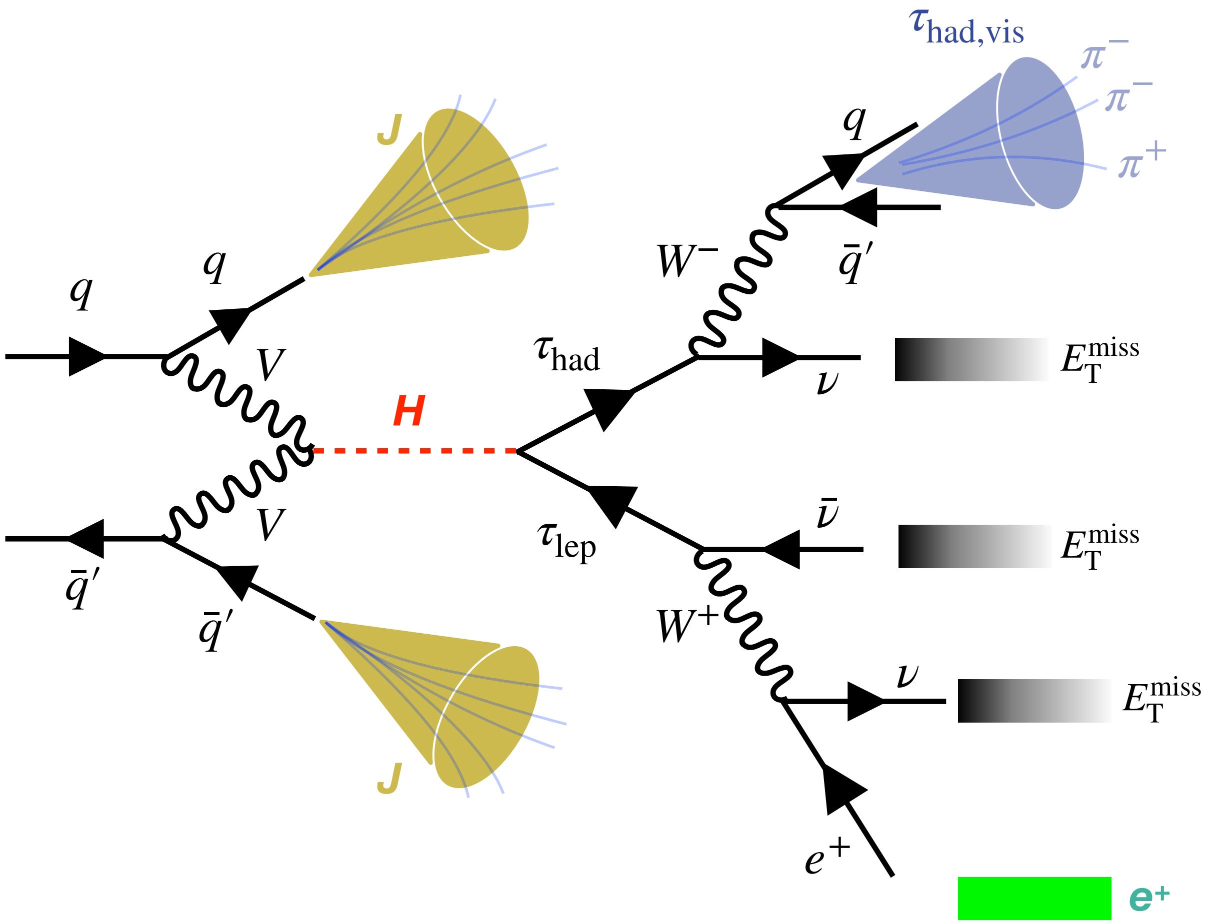


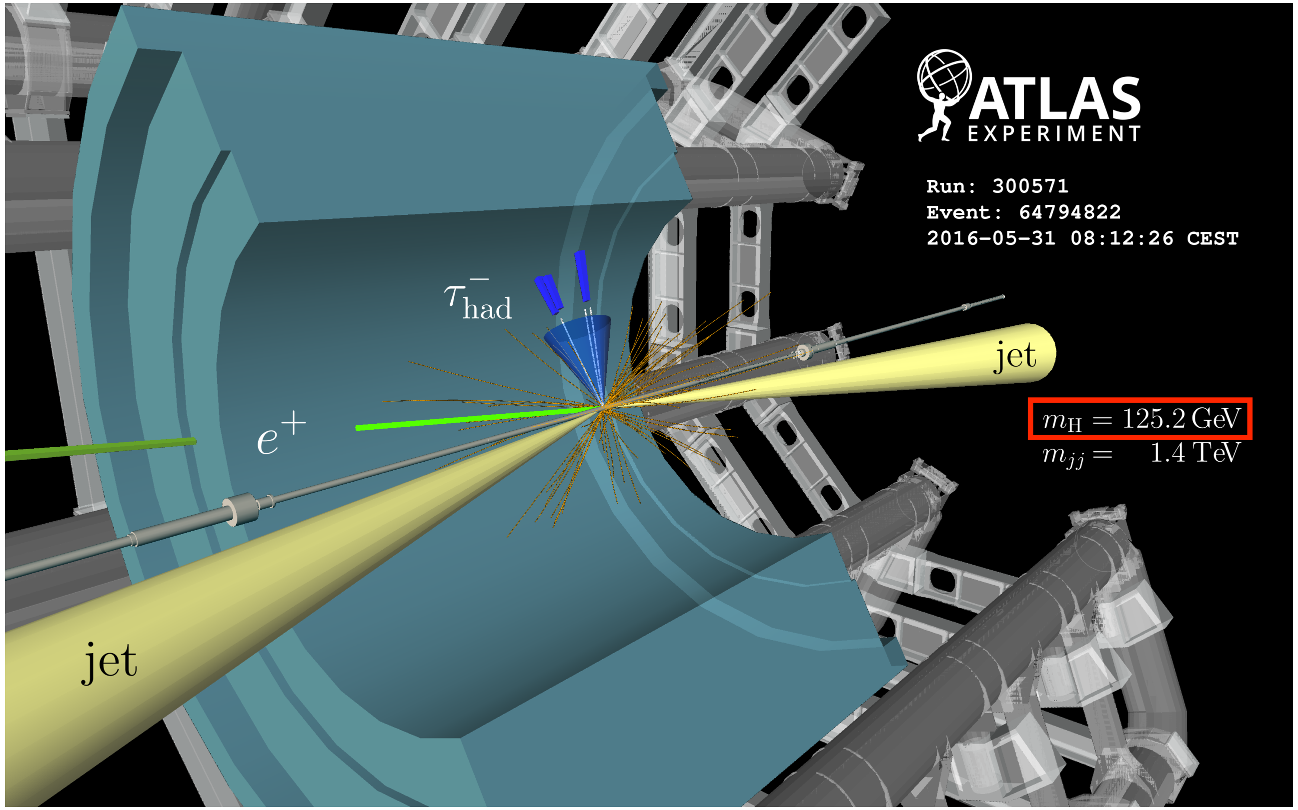


arXiv: 1811.08856, modified

# Content

Evidence for V($\ell$)H($\tau\tau$) production in $H \to \tau_{\rm lep}\tau_{\rm had}$ and $H \to \tau_{\rm had}\tau_{\rm had}$ channels

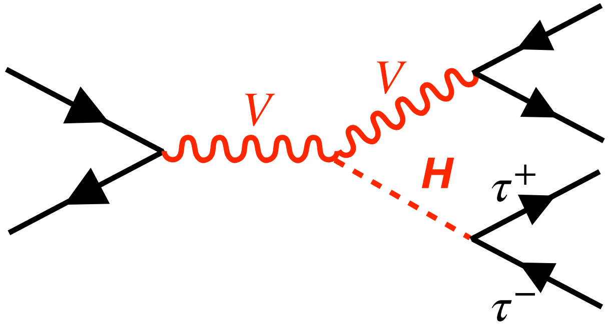


NEW

Measurement of CP properties using $H \to \tau_{\rm lep}\tau_{\rm had}$ and $H \to \tau_{\rm had}\tau_{\rm had}$ decay products

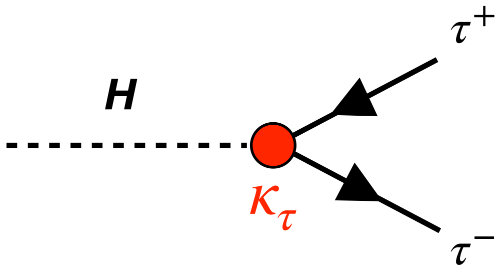


Eur. Phys. J. C 83, 563 (2023)

Search for LFV in $H \to \ell\tau_{\rm lep}$ and $H \to \ell\tau_{\rm had}$ final states

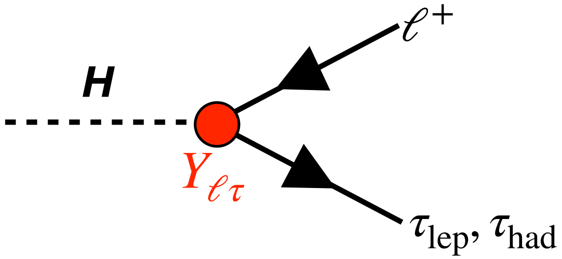


JHEP 07 (2023) 166

- Very simplified description of analysis details and results
- For more: Backup, links or offline in-person


Some other related ATLAS results:

Non-resonant $HH \to b\bar{b}\tau\tau$

See Guiseppe's talk

$H \to \tau\tau$ couplings

VBF $H \to \tau\tau$ CP

# Evidence for *VH*, $H \rightarrow \tau\tau$ Process - Motivation and Strategy

**Goal: measure the σ x BR of V($\ell$)H($\tau\tau$) production, one of the major Higgs production modes. V($\ell$)H($b\bar{b}$) observed[1] in 2018**

- ***V* = {*W, Z*} production modes with decays into light leptons ($\ell = e$ or $\mu$) → Ambiguities due to multiple $\ell / \nu$ sources**

**Assign leading $p_T$ $\ell$ to V decays and require opposite-sign $\tau_{\rm lep}\tau_{\rm had}$ / $\tau_{\rm had}\tau_{\rm had}$**

### *WH*

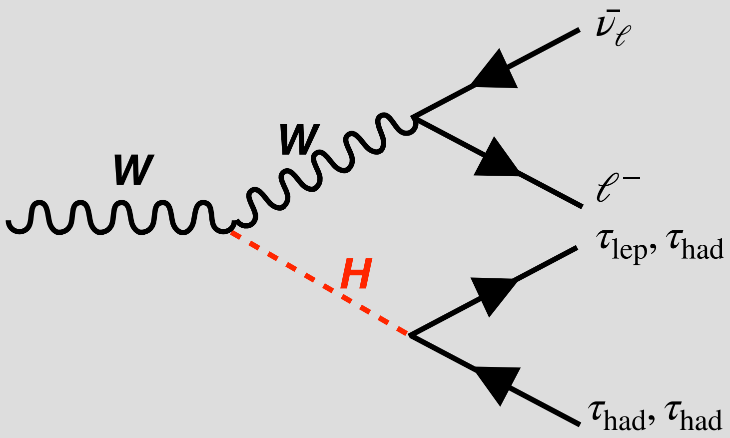


Suppress *Z+jets* in $\tau_{\rm lep}\tau_{\rm had}$ channel by requiring 2 same-sign $\ell$

Enhance *H* sensitivity with a mass-window of 60/80 < $M_{2T}$ < 130 GeV
→ Multiple (*H* & *W*) neutrino sources

Transverse-projection (T) two parent (2) "transverse mass" variable $M_{2T}$ [2]

### *ZH*

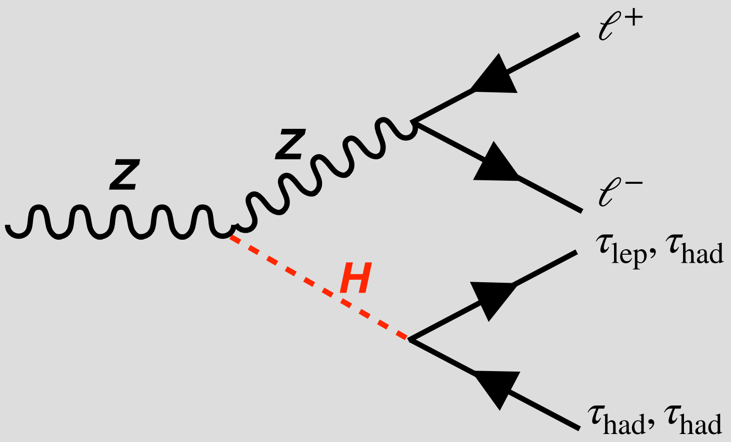


Select *Z* bosons with requiring 81/71 < $m_{\ell^+\ell^-}$ < 101/111 GeV
→ 3$\ell$ in $\tau_{\rm lep}\tau_{\rm had}$. Assign largest $p_T^\ell$ with best $m_Z$

Enhance *H* sensitivity with a mass-window of 100 < $m_{MMC}$ < 170/180 GeV

**Neural Networks (NN) are used (Run-1: no MVA) to separate signal from the dominant diboson (VV = WZ, ZZ) backgrounds**

- **One NN is trained in each channel, except $WH\tau_{\text{lep}}\tau_{\text{had}}$, which has three: $ee$, $e\mu$ and $\mu\mu$**
- **Misidentified jets are estimated using the data-driven Fake-Factor method**

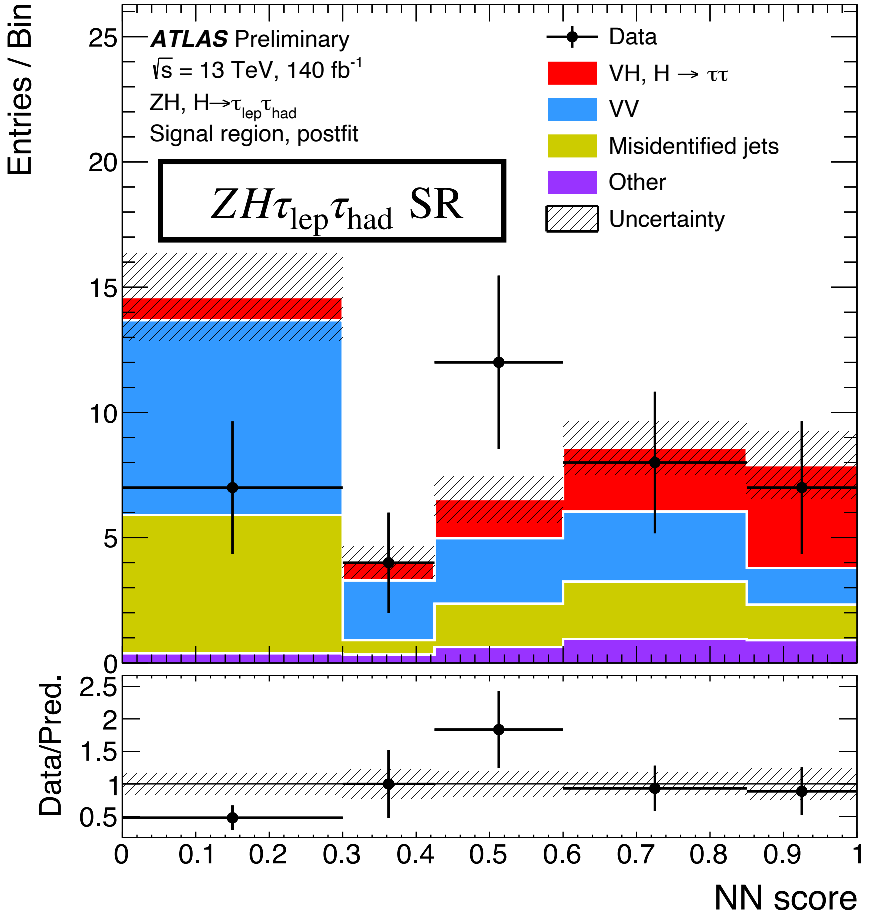


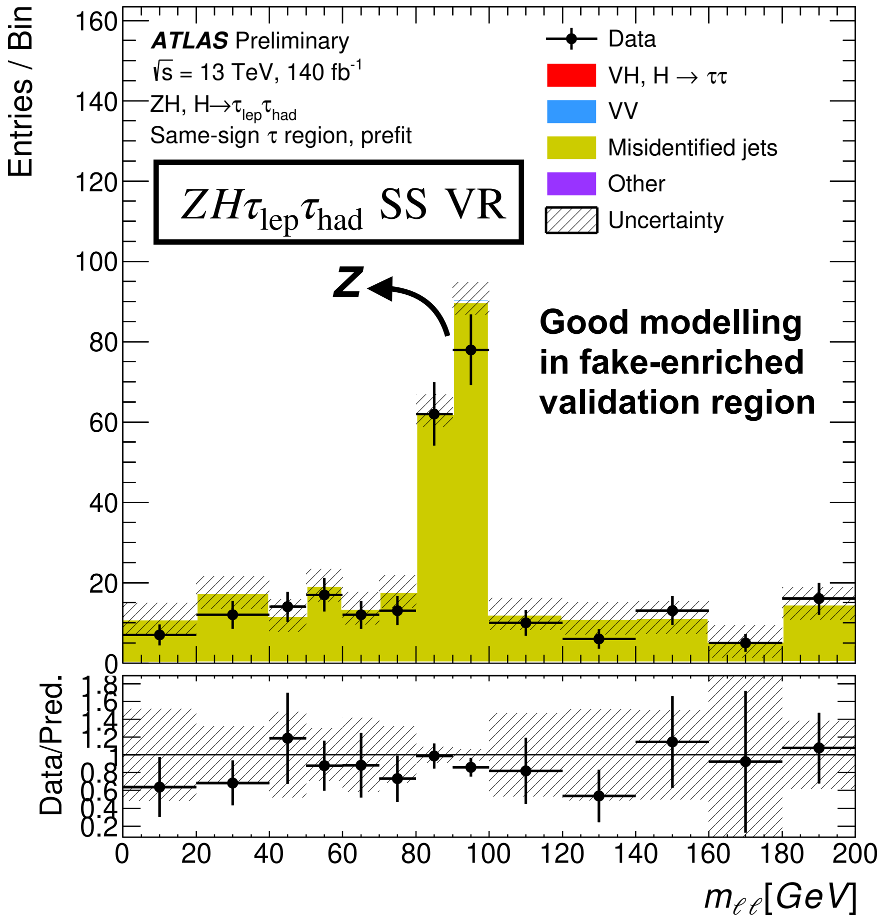

**Four signal region NN distributions are used in a binned profile likelihood fit to extract the parameter of interest (PoI)** $\mu_{VH}^{\tau\tau} = \frac{\sigma}{\sigma_{SM}}$

- **No control regions in the fit → Thorough checks are done to validate the background modelling**
- **Main results from 1 PoI fit:** $\mu_{VH}^{\tau\tau} = \mu_{WH}^{\tau\tau} = \mu_{ZH}^{\tau\tau} = 1.28^{+0.39}_{-0.36}$ **(2 PoI fit:** $\mu_{WH}^{\tau\tau} = 1.48^{+0.56}_{-0.50}$ **and** $\mu_{ZH}^{\tau\tau} = 1.09^{+0.51}_{-0.44}$ **→ compatible)**

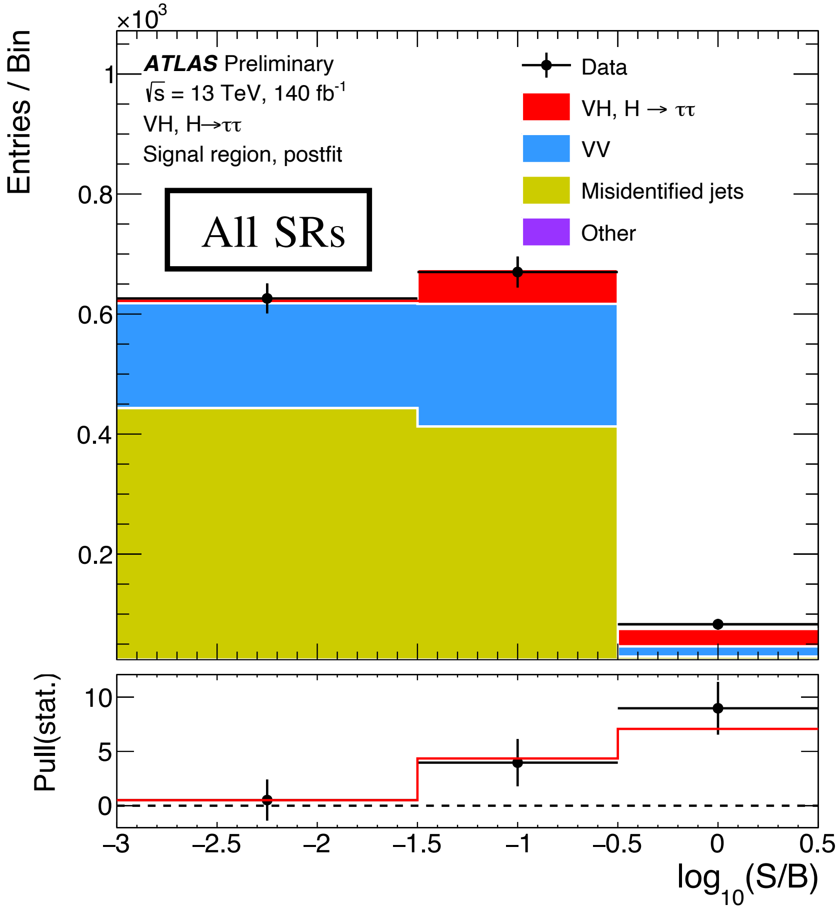


| Source of uncertainty | $\delta\mu/\mu_{\mathrm{VH}}^{\tau\tau}$ [%] |
|---|---|
| Hadronic $\tau$–lepton decay | 10 |
| Background sample size | 9 |
| Misidentified jets | 5 |
| Jet and $E_{\mathrm{T}}^{\mathrm{miss}}$ | 5 |
| Theoretical uncertainty in signal | 5 |
| Theoretical uncertainty in top-quark, $VV$ and $VVV$ processes | 4 |
| Electrons and muons | 2 |
| Luminosity | 1 |
| Flavour tagging | < 1 |
| Total systematic uncertainty | 17 |
| Total statistical uncertainty | 24 |
| Total | 29 |

**Four signal region NN distributions are used in a binned profile likelihood fit to extract the parameter of interest (PoI)** $\mu_{VH}^{\tau\tau} = \frac{\sigma}{\sigma_{SM}}$

- **No control regions in the fit → Thorough checks are done to validate the background modelling**
- **Main results from 1 PoI fit:** $\mu_{VH}^{\tau\tau} = \mu_{WH}^{\tau\tau} = \mu_{ZH}^{\tau\tau} = 1.28^{+0.39}_{-0.36}$ **(2 PoI fit:** $\mu_{WH}^{\tau\tau} = 1.48^{+0.56}_{-0.50}$ **and** $\mu_{ZH}^{\tau\tau} = 1.09^{+0.51}_{-0.44}$ **→ compatible)**

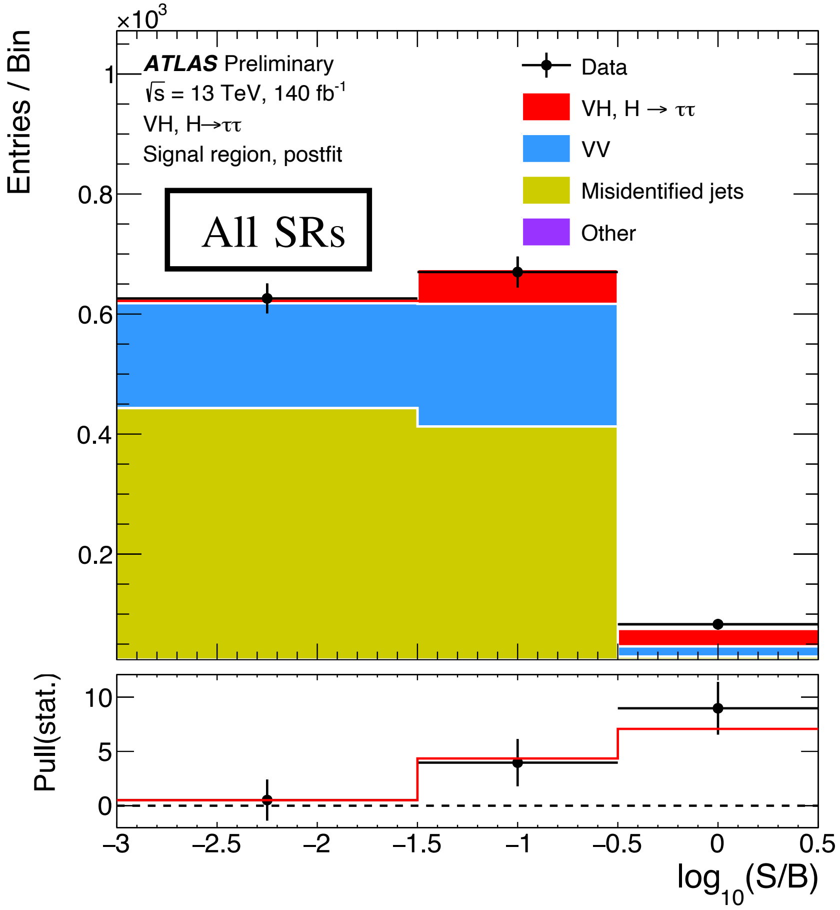


| Source of uncertainty | $\delta\mu/\mu_{\mathrm{VH}}^{\tau\tau}$ [%] |
|---|---|
| Hadronic $\tau$–lepton decay | 10 |
| Background sample size | 9 |
| Misidentified jets | 5 |
| Jet and $E_{\mathrm{T}}^{\mathrm{miss}}$ | 5 |
| Theoretical uncertainty in signal | 5 |
| Theoretical uncertainty in top-quark, *VV* and *VVV* processes | 4 |
| Electrons and muons | 2 |
| Luminosity | 1 |
| Flavour tagging | < 1 |
| Total systematic uncertainty | 17 |
| Total statistical uncertainty | 24 |
| Total | 29 |

**Observed (Expected) Significance: 4.2σ (3.6σ)**

Previous ATLAS[1] : (20.3 $\mathrm{fb}^{-1}$, 8 TeV) $\mu_{inc.}^{\tau\tau} < 5.5 \times \mathrm{SM}\,@\,95\,\%\,\mathrm{CL}$

Latest CMS[2] : (138 $\mathrm{fb}^{-1}$, 13 TeV) $\mu_{inc.}^{\tau\tau} = 1.79 \pm 0.45$

# Higgs → $\tau\tau$ Decay CP - Motivation & Strategy

**According to Sakharov Conditions[1], new sources of CP-violation might explain the baryon asymmetry in the universe**

- **CP-mixing alters the transverse-spin correlations between $\tau$-particles → changes carried over to the $\tau$-decay products**

**Theory: Parametrize $\kappa_\tau$ with a CP-mixing parameter $\phi_\tau$**

$$\mathscr{L}_{H\tau\tau} = -\frac{m_\tau}{v}\kappa_\tau(\cos\phi_\tau\bar{\tau}\tau + \sin\phi_\tau\bar{\tau}i\gamma_5\tau)H$$

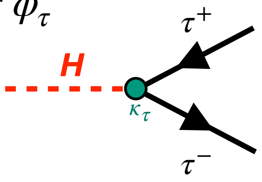


$\phi_\tau = 0^\circ$ → Pure CP-even (Scalar)

$\phi_\tau = 90^\circ$ → Pure CP-odd (Pseudo-scalar)

**Observable: Signed acoplanarity angle $\phi^*_{CP}$ between $\tau$-decay planes**

$$d\Gamma_{H\rightarrow\tau^+\tau^-} \propto \text{constant} - \cos(\phi^*_{CP} - 2\phi_\tau)$$

**CP-mixing = phase-shift in $\phi^*_{CP}$**

Eur. Phys. J. C 83, 563 (2023)

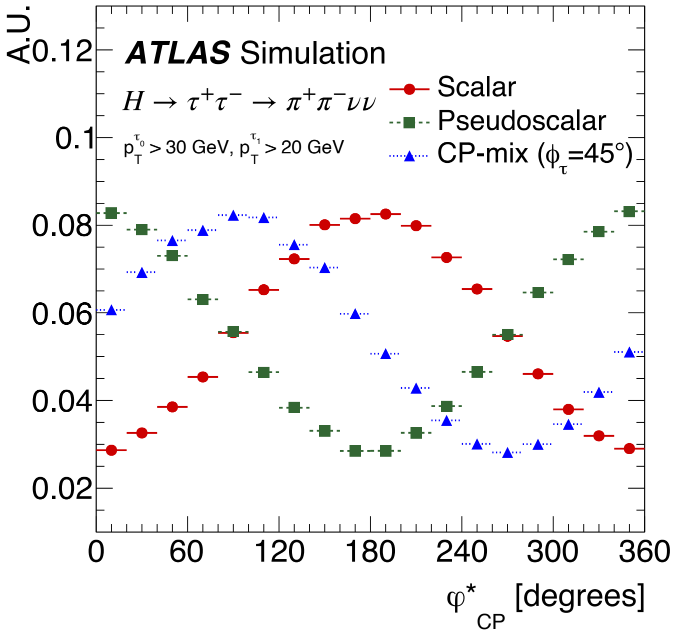


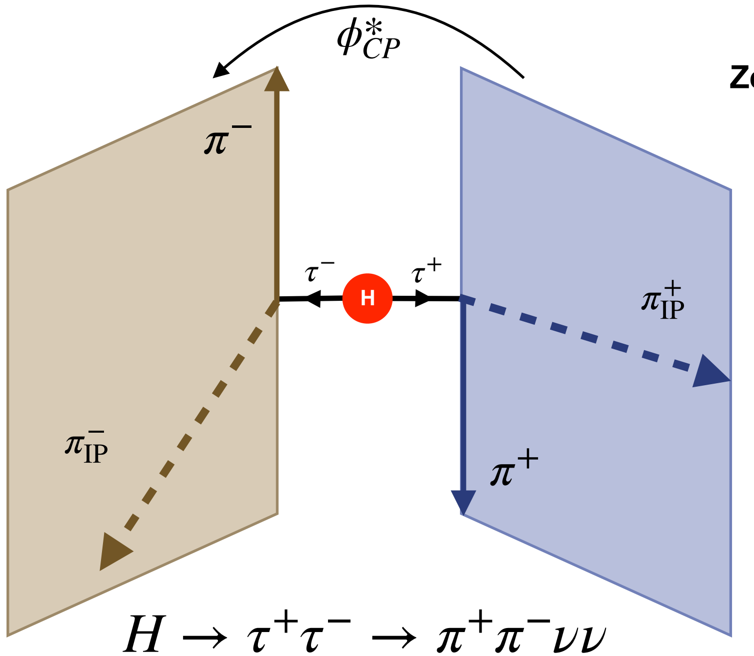


**Zero-momentum-frame (ZMF) of di-$\tau_{vis}$ ~ rest frame of *H***

$$H \rightarrow \tau^+\tau^- \rightarrow \pi^+\pi^-\nu\nu$$

# Higgs → $\tau\tau$ Decay CP - Analysis Regions

**$\tau_{\text{lep}}\tau_{\text{had}}$ and $\tau_{\text{had}}\tau_{\text{had}}$ final states are broken down to further regions according to decay modes and topologies**

- **8 (4 regions x 2 final states) inclusive SRs have 8 corresponding $Z \to \tau\tau$ CRs. +2 $Z$ CRs to constrain $\pi^0$ energy resolution**
- **SRs are further split into 3 subregions of increasingly optimised $\phi^*_{CP}$ sensitivity (low/medium/high)**

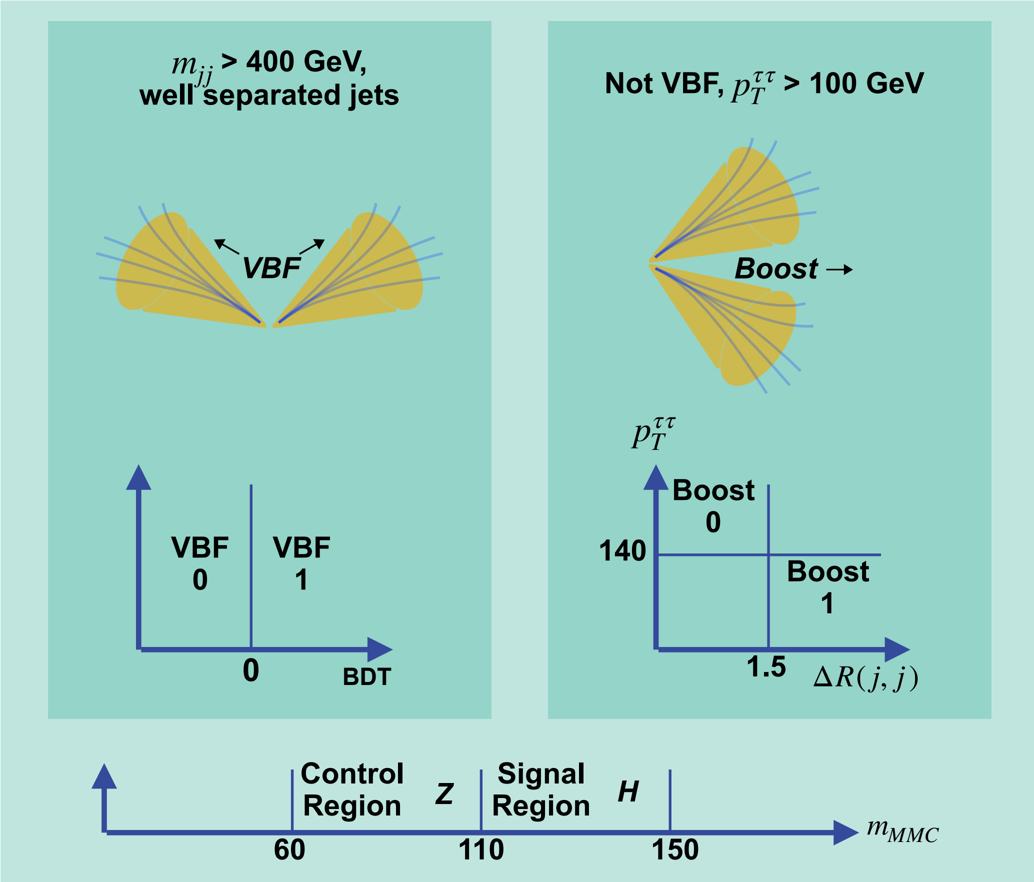


**Misidentified jets:**
**Fake-Factor method**

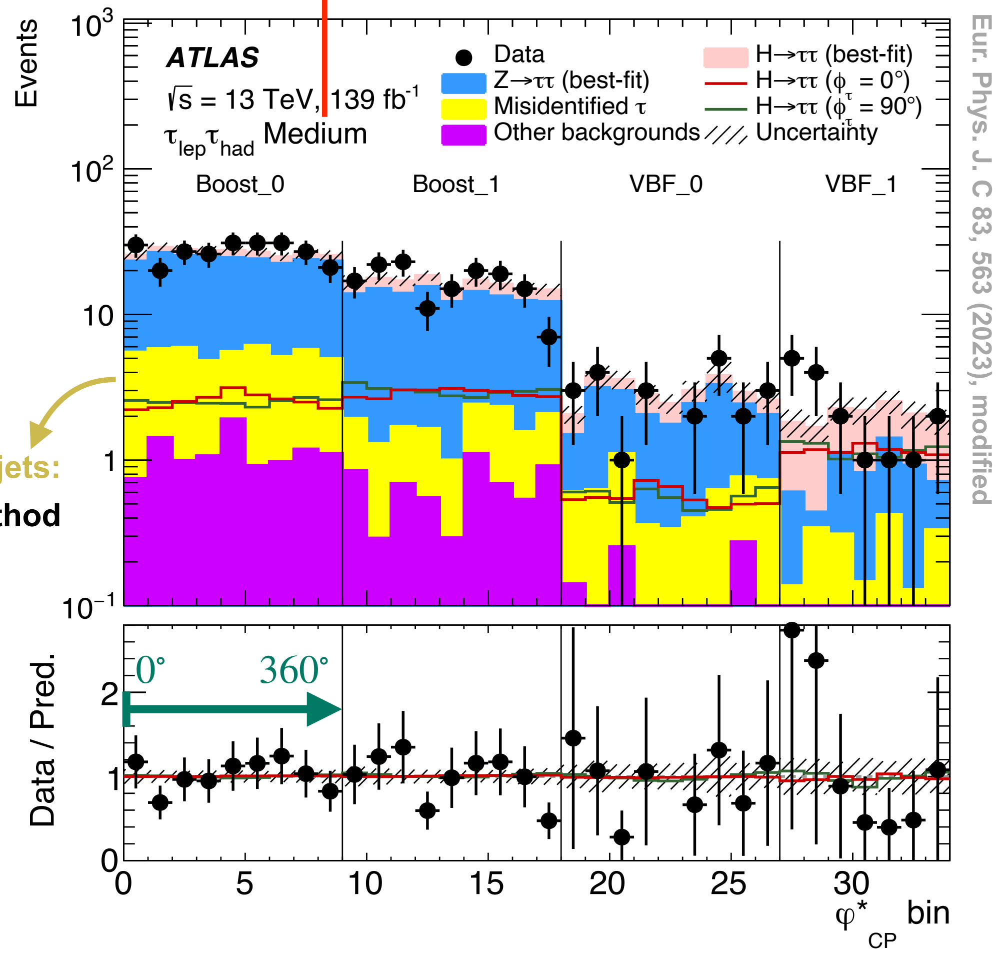


**BDT = Boosted Decision Tree, optimized[1] to tag VBF events**

# Higgs → $\tau\tau$ Decay CP - Results

**Using $\phi_\tau$ as the PoI, a binned profile likelihood fit is evaluated using all signal and control regions**

- **Analysis is statistically limited, among systematics, Jet Energy Scale/Resolution had the highest impact on $\phi_\tau$ with $3.4^\circ/2.5^\circ$**

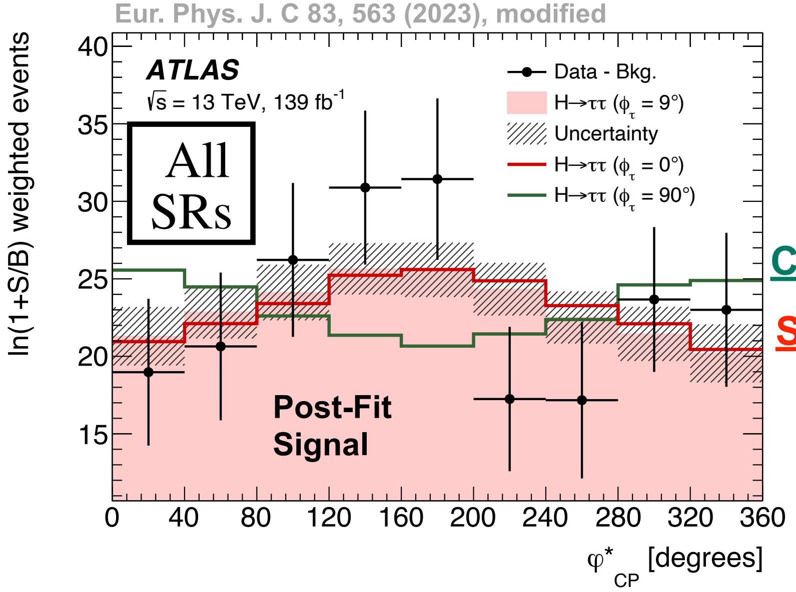


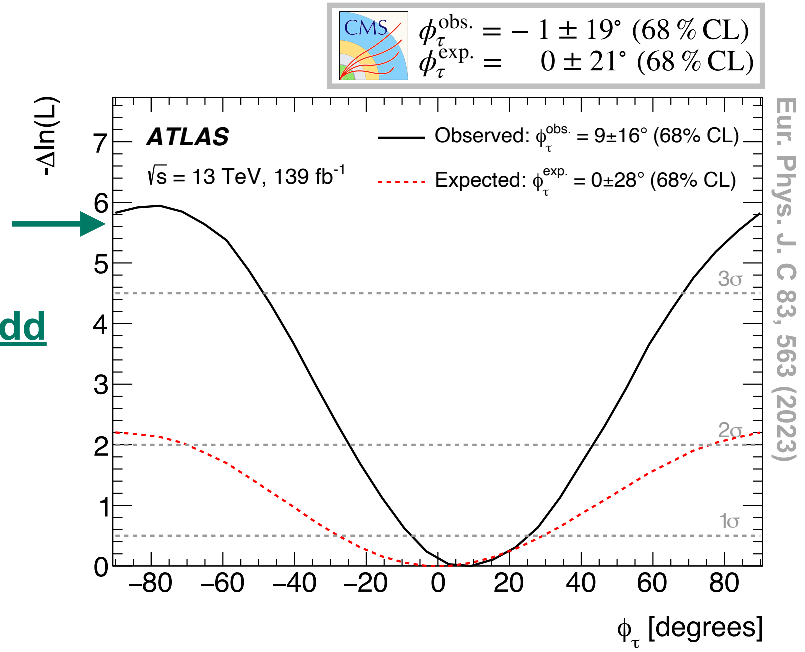


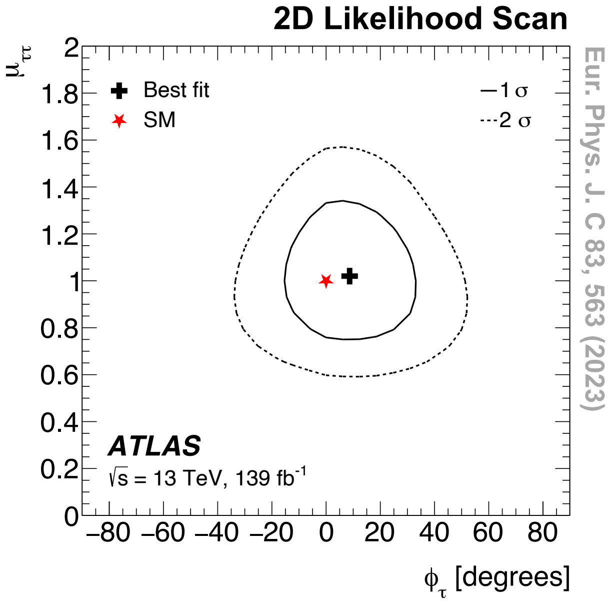


**SM Higgs normalization is left unconstrained →Using only the shape**

$\phi_\tau^{obs.}$ $(\phi_\tau^{exp.}) = 9 \pm 16^\circ$ $(0 \pm 28^\circ)$

**Pure CP-odd hypothesis is rejected with 3.4σ (CMS: 3σ)**

**Agreement with SM within 1σ**
**No strong correlations observed**

**First ATLAS result**

# Higgs → $\ell\tau$ LFV Search - Strategy & Backgrounds

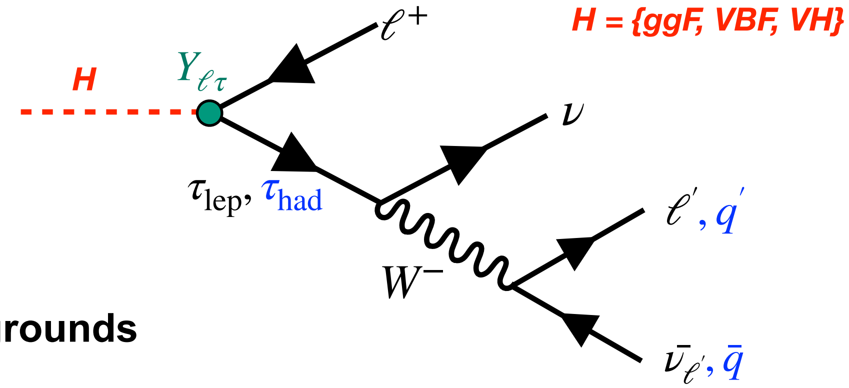


**Search for Lepton-Flavour-Violation (LFV) in H → $e\tau$ & H → $\mu\tau$ decays ($p_T^\ell$ ordered)**

- **$\ell, \tau_{lep}$ and $\ell, \tau_{had}$ channels are further split into VBF ($N_j > 2$) & non-VBF regions**
- **Misidentified objects: data-driven Fake-Factor or ABCD methods**
- **MC Template (Symmetry) method is used to estimate $Z \to \tau\tau$ & Top (All) SM backgrounds**

**MC Template (both channels)**

**Shape: From MC simulation "template"**

**Normalization: From a data-fit in a CR**

**CRs are high in purity and show good modelling already at the Pre-fit level**

JHEP 07 (2023) 166, modified

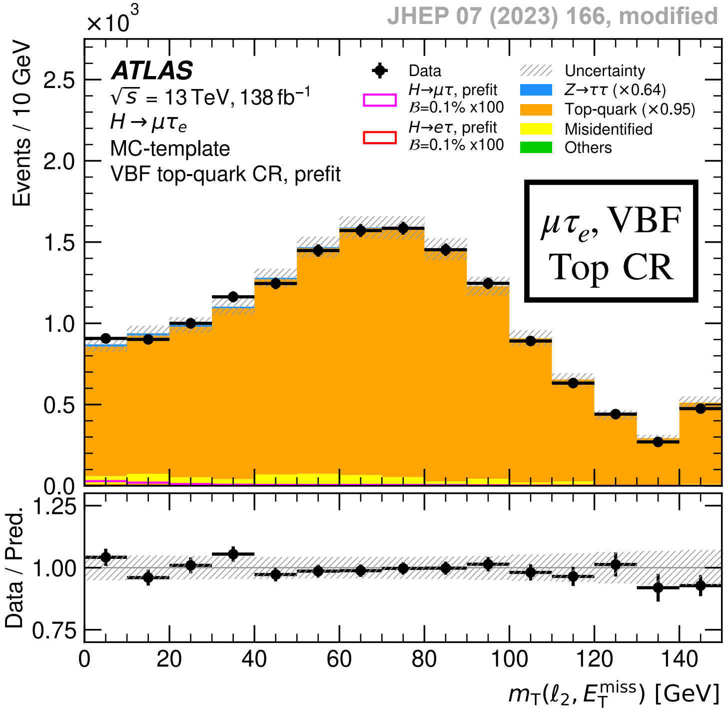


JHEP 07 (2023) 166, modified

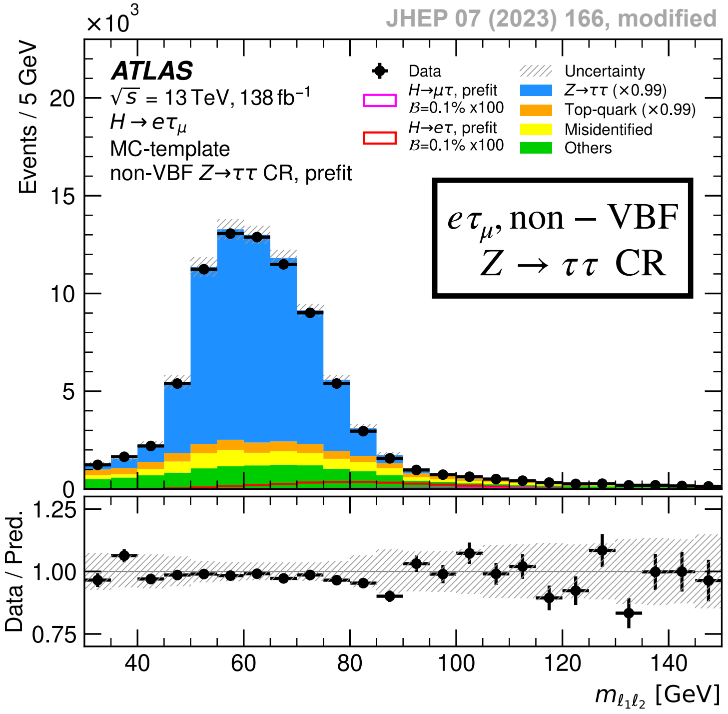

# Higgs → $\ell\tau$ LFV Search - Symmetry Method

- **Estimate backgrounds in a channel ($e\tau$/$\mu\tau$) using the data events from the selection of the other channel ($\mu\tau$/$e\tau$)**
  - **Assumption 1: $e \longleftrightarrow \mu$ exchange is symmetric in SM background processes**
  - **Assumption 2: LFV signal processes are asymmetric i.e. BR(H → $e\tau$) $\neq$ BR(H → $\mu\tau$). Method is sensitive to $\Delta$BR**
  - **Asymmetries originating from instrumental effects (detector efficiency, fake rates) has to be corrected**

JHEP 07 (2023) 166, modified

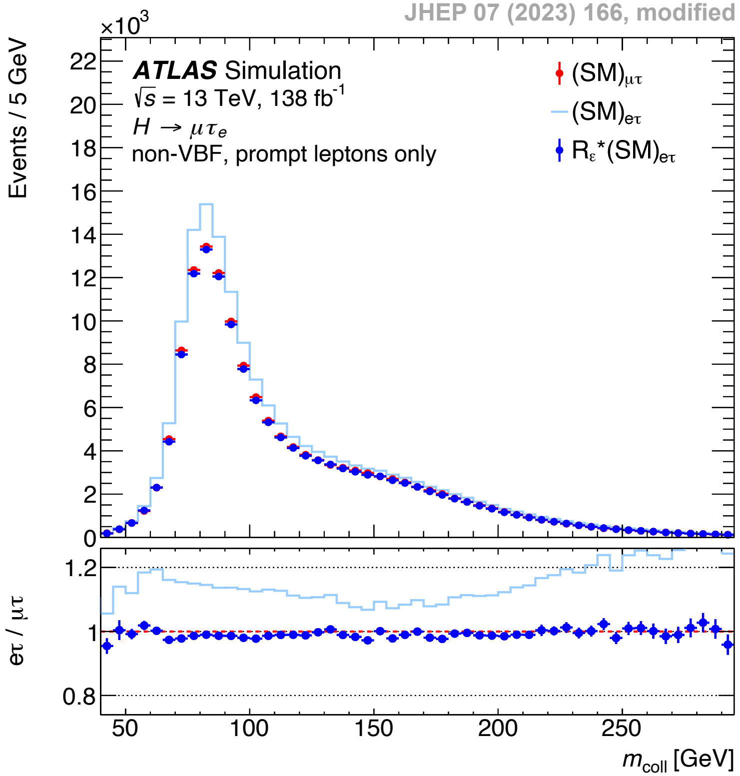


**After efficiency correction**

$\mathrm{SM}(e\tau) \rightarrow \mathrm{R}_\epsilon \times \mathrm{SM}(e\tau)$

**corrected $e\tau$ background models $\mu\tau$ background well**

JHEP 07 (2023) 166, modified

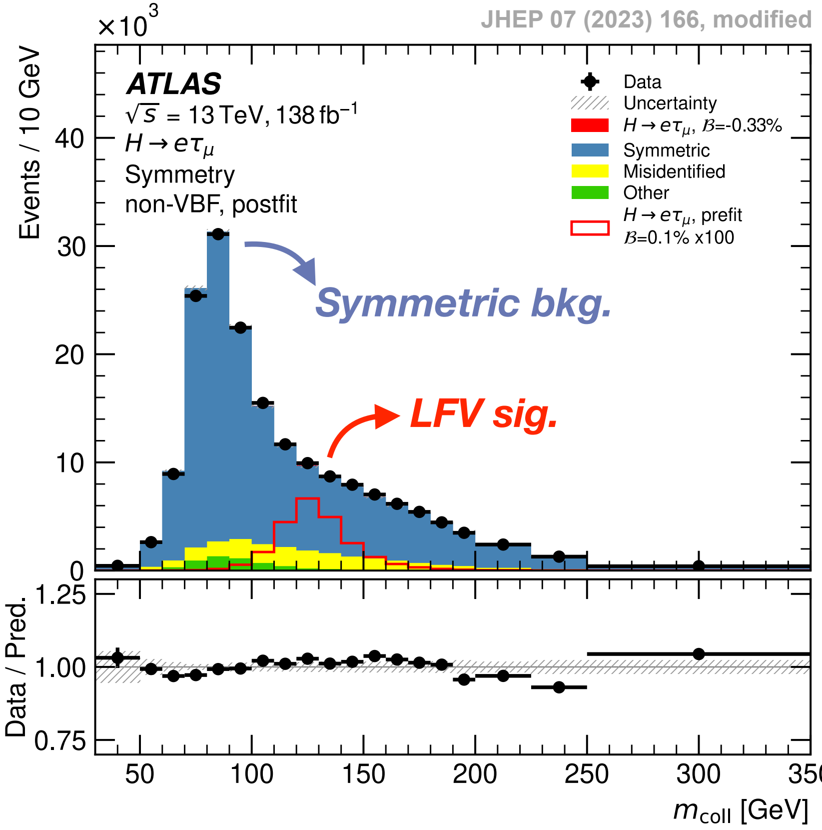

# Higgs → $\ell\tau$ LFV Search - Results

New

**Taking LFV decay BRs as PoIs, 1 PoI (SYM+MCT) and 2 PoI (MCT) binned profile likelihood fits are performed on SRs + CRs**

- **Analysis is systematically limited, background sample size & misidentified background uncertainties are dominant**

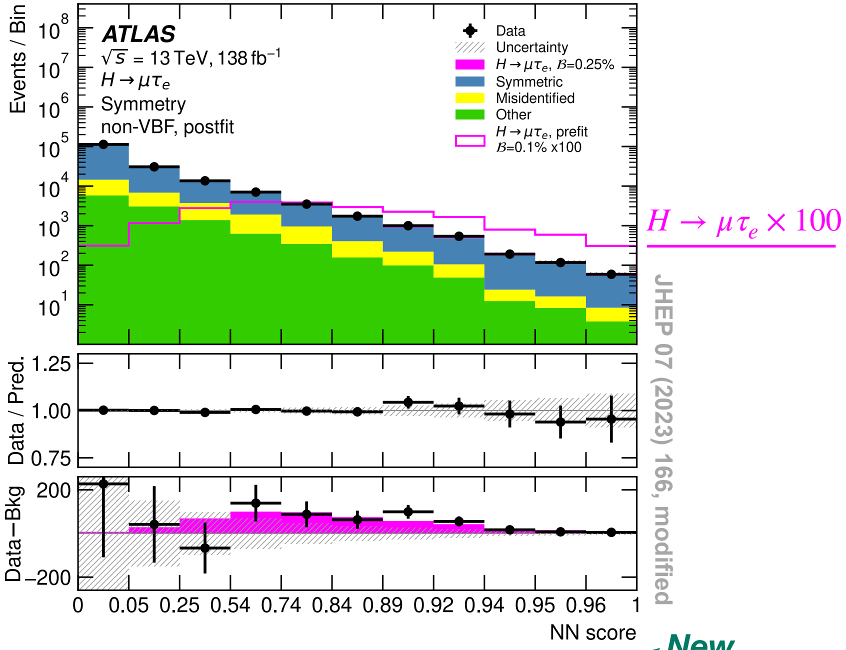


New

**SRs: Multi-classifier BDTs and NNs**
**Fit to discriminant score distributions**

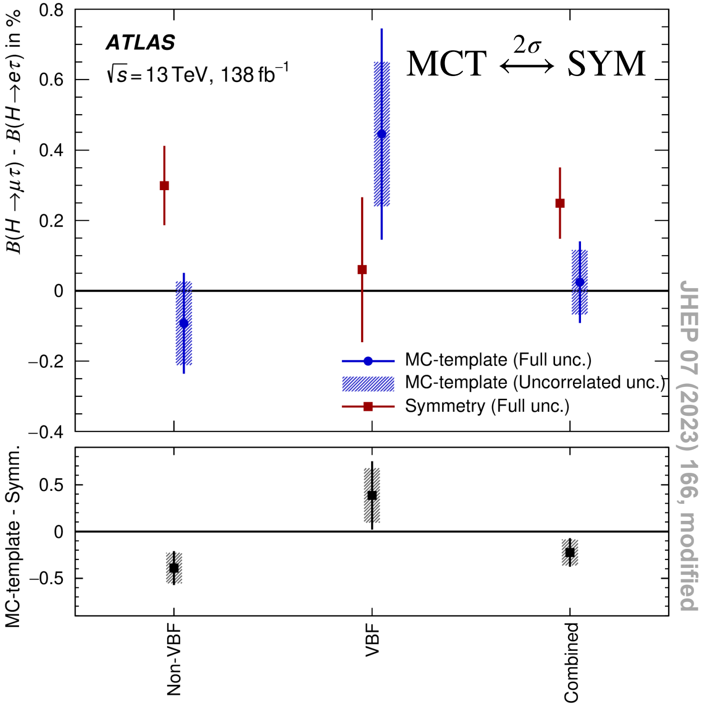


**ΔBR = BR(H → $\mu\tau$) - BR(H → $e\tau$)**

**ΔBR MCT ($\mu\tau_e$+$e\tau_\mu$) = (0.02 ± 0.12)%**
**ΔBR SYM ($\ell\tau_{lep}$) = (0.25 ± 0.10)%**

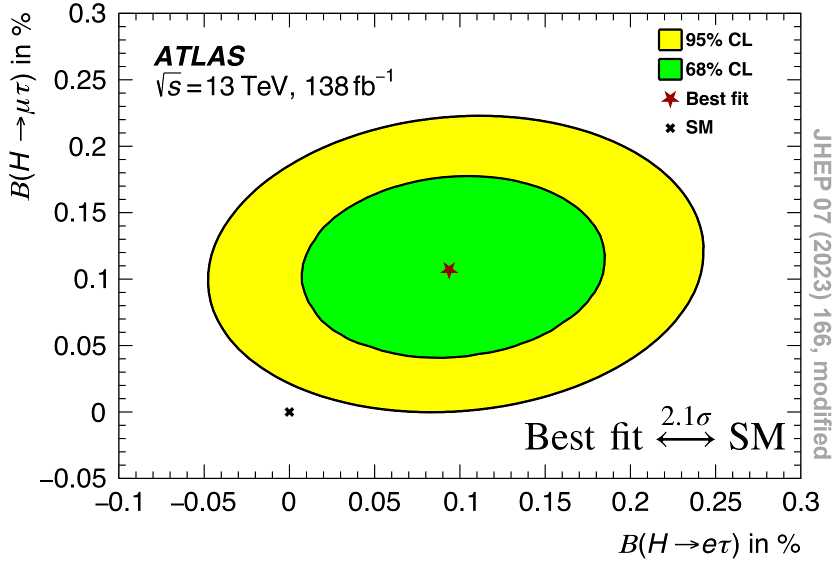


**MCT ($\ell\tau_{lep}$+$\ell\tau_{had}$)**

**New best**

**BR(H → $e\tau$) < 0.20% (0.11%) @ 95% CL**
**BR(H → $\mu\tau$) < 0.18% (0.09%) @ 95% CL**

**Previous stringest direct limits ($e\tau$, $\mu\tau$)**
**36 fb$^{-1}$, 13 TeV ATLAS[1] (0.47%, 0.28%)**
**137 fb$^{-1}$, 13 TeV CMS[2] (0.22%, 0.15%)**

# Summary and Outlook

- **First evidence (4.2σ) for V($\ell$)H($\tau\tau$) production (NNs, x7 data)**
- **Decay CP angle $\phi_\tau^{\text{obs.}} = 9 \pm 16^\circ$ consistent with the SM within 1σ (First ATLAS result)**
- **Stringest LFV BR(H → $e\tau$) = 0.2% @ 95%CL, 2σ overall compatibility with SM (x4 data, 2PoI fit, NNs)**

**More data, better hardware and improved algorithms → High hopes!**

**Run-3 (2022-25) = 2 x Run-2 data**

**$\tau_{\text{had}}$ decay-mode classifier example:**
**BDT → DeepSet NN brings +9% efficiency[1]**

**High-Luminosity LHC (2029-) = 3000 fb$^{-1}$**

**LFV Analysis Example for BR(H → $\ell\tau$) = 0.1%:**
**8.1σ expected sensitivity → Four times better than Run-2 result!**

ATL-PHYS-PUB-2022-054

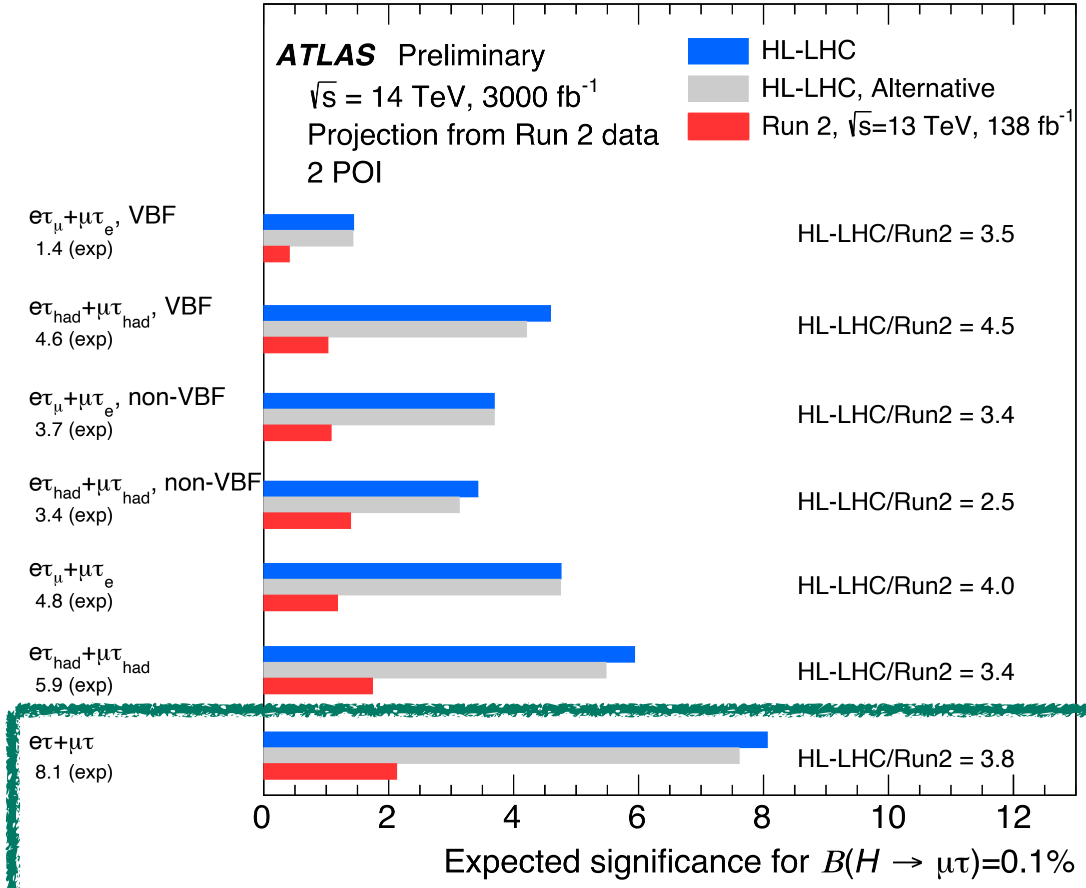


Thank you for your attention!
Uncertainties,
detector resolution,
backgrounds
LHC
ATLAS
EXPERIMENT
SM

# Backup

# LHC and ATLAS

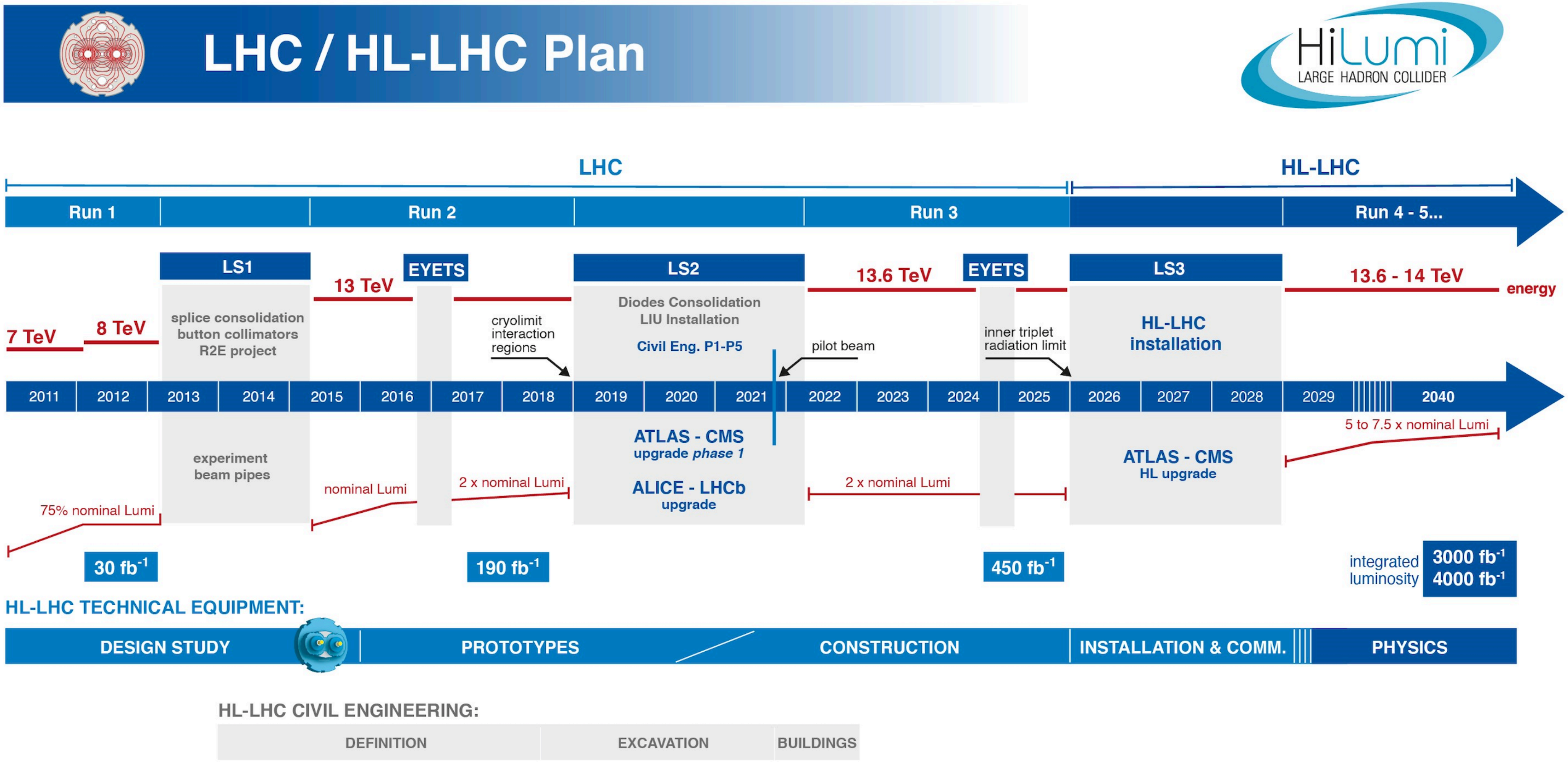


*Image Credit: CERN*

Reconstruction:
Anti-kt jet algorithm, R=0.4
Prong count by defining core and isolation tracks using BDTs with tracks with dR=0.4 of tau axis
Using: pT, tracker hits, impact parameters
Number of core tracks give the prongness

Energy calibration:
Apply pile-up and energy cluster correction to objects within R=0.2 of the tau candidate
Use corrected energy with a boosted regression tree to calculate final energy

Gamma* -> tautau (signal) vs. Dijet (bkg.)

| Working point | Signal efficiency 1-prong | 3-prong | Background rejection BDT 1-prong | 3-prong | Background rejection RNN 1-prong | 3-prong |
|---|---|---|---|---|---|---|
| Tight | 60% | 45% | 40 | 400 | 70 | 700 |
| Medium | 75% | 60% | 20 | 150 | 35 | 240 |
| Loose | 85% | 75% | 12 | 61 | 21 | 90 |
| Very loose | 95% | 95% | 5.3 | 11.2 | 9.9 | 16 |

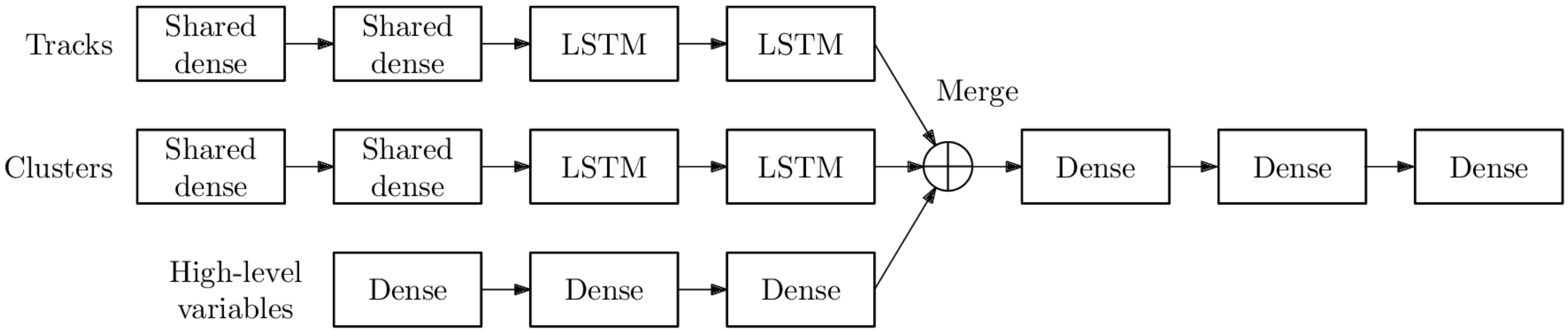


LSTM (Long Short-Term Memory)

# ATLAS - Tau Identification in ATLAS

| | Observable | 1-prong | 3-prong |
|---|---|---|---|
| Track inputs | $p_T^{\text{seed jet}}$ | • | • |
| | $p_T^{\text{track}}$ | • | • |
| | $\Delta\eta^{\text{track}}$ | • | • |
| | $\Delta\phi^{\text{track}}$ | • | • |
| | $\|d_0^{\text{track}}\|$ | • | • |
| | $\|z_0^{\text{track}} \sin\theta\|$ | • | • |
| | $N_{\text{IBL hits}}$ | • | • |
| | $N_{\text{Pixel hits}}$ | • | • |
| | $N_{\text{SCT hits}}$ | • | • |
| Cluster inputs | $p_T^{\text{jet seed}}$ | • | • |
| | $E_T^{\text{cluster}}$ | • | • |
| | $\Delta\eta^{\text{cluster}}$ | • | • |
| | $\Delta\phi^{\text{cluster}}$ | • | • |
| | $\lambda_{\text{cluster}}$ | • | • |
| | $\langle\lambda^2_{\text{cluster}}\rangle$ | • | • |
| | $\langle r^2_{\text{cluster}}\rangle$ | • | • |
| High-level inputs | $p_T^{\text{uncalibrated}}$ | • | • |
| | $f_{\text{cent}}$ | • | • |
| | $f^{-1}_{\text{leadtrack}}$ | • | • |
| | $\Delta R_{\text{max}}$ | • | • |
| | $\|S_{\text{leadtrack}}\|$ | • | |
| | $S_T^{\text{flight}}$ | | • |
| | $f_{\text{iso}}^{\text{track}}$ | • | • |
| | $f_{\text{track}}^{\text{EM}}$ | • | • |
| | $p_T^{\text{EM+track}}/p_T$ | • | • |
| | $m^{\text{EM+track}}$ | • | • |
| | $m^{\text{track}}$ | | • |

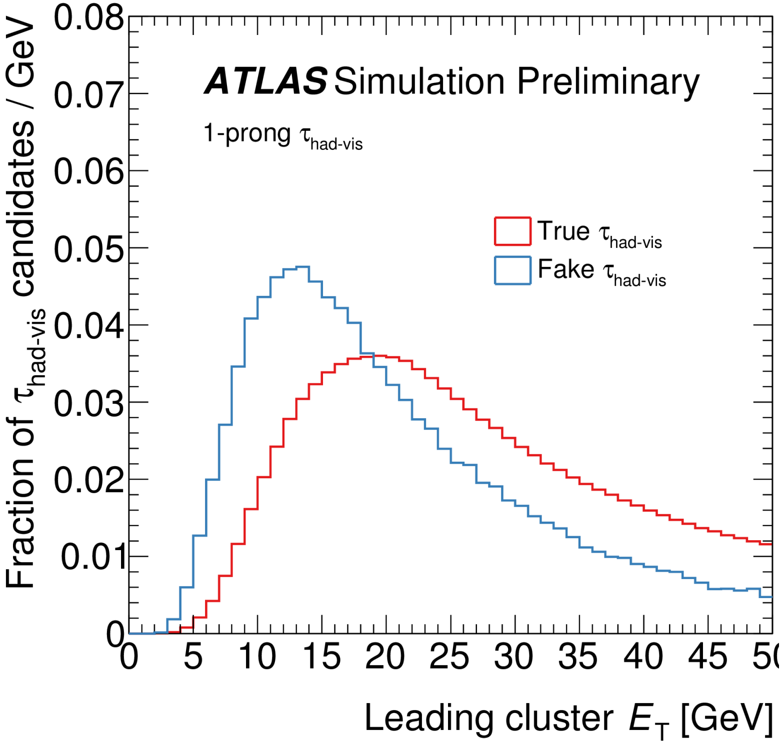


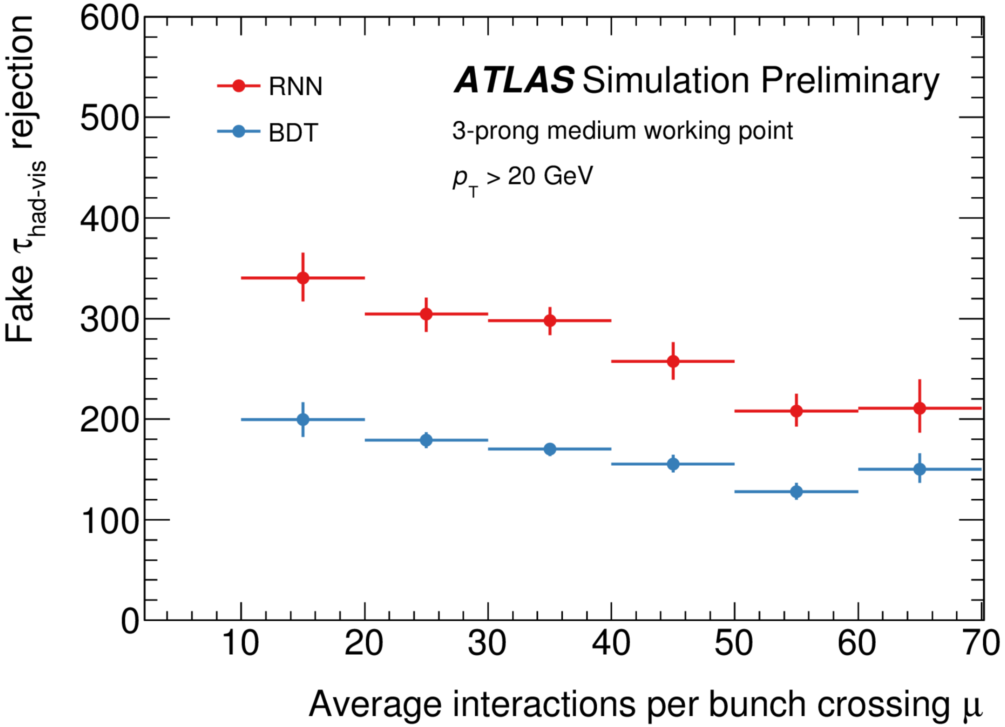

- Originally developed by the CDF collaboration at Tevatron $\rightarrow$ adopted by the ATLAS experiment.
- Accounts for the kinematic constraints while considering the variation of energy and position of the particles in the decay cascades over the allowed phase space.
  - Assumes neutrinos are the only $E_{\mathrm{T}}^{\mathrm{miss}}$ source.
  - For each event, scan over possible configurations of the visible and invisible $\tau$-decay products is performed in a Markov chain.
  - For each kinematic configuration, the final weight is defined as a log-likelihood of its total probability.
- The solution with the highest likelihood and largest weight is set as a final estimator of $m_H$.

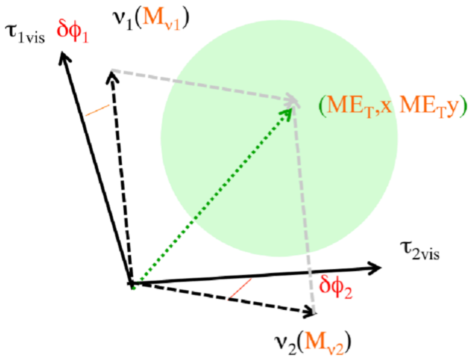


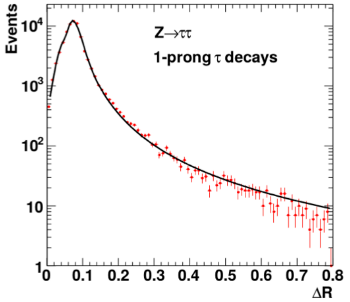


**Figure:** Example of the probability distribution functions $P(\Delta R, p_\tau)$ [3] at a particular $p_\tau$.

$$\mathcal{L} = -\log(\mathcal{P}_{\mathrm{total}}) = -\log(\mathcal{P}(\Delta R_{\mathrm{vis,miss\ 1,p_{\tau\ 1}}}) \times \mathcal{P}(\Delta R_{\mathrm{vis,miss\ 2,p_{\tau\ 2}}}) \times \mathcal{P}(\not{E}_{\mathrm{T\ x,y}}) \times \mathcal{P}(E_{\mathrm{vis.}\ \tau\ 1}) \times \mathcal{P}(E_{\mathrm{vis.}\ \tau\ 2})) \times \mathcal{P}(m_{\mathrm{miss\ 1}}) \times \mathcal{P}(m_{\mathrm{miss\ 2}})$$

probability of the topology at a given point | angular distance b/w (vis.,mis.) decay products | MET | τ-lepton kinematics | invariant mass of neutrinos (in case of $\tau_{lep}$)

https://indico.cern.ch/event/796574/contributions/3521687/attachments/1917917/3172786/The_status_of_Missing_Mass_Calculator_for_Higgs_boson_mass_estimation_in_the_ATLAS_H___analysis18.pdf

# VH

# VH

| Process | MC Generator + UEPS | PDF Set | Perturbative Order |
|---|---|---|---|
| Signal | | | |
| $W \to \ell\nu, H \to \tau\tau$ | Powheg [21–25]+Pythia8.235 [31] | PDF4LHC15NLO [37] | NLO |
| $Z \to \ell\ell, H \to \tau\tau$ | Powheg+Pythia8.235 | PDF4LHC15NLO | NLO |
| Background | | | |
| ggF $H \to \tau\tau$ | Powheg+Pythia8.235 | PDF4LHC15NLO | NNLO |
| VBF $H \to \tau\tau$ | Powheg+Pythia8.235 | PDF4LHC15NLO | NLO |
| $t\bar{t}H, H \to \tau\tau$ | Powheg+Pythia8.235 | NNPDF30NNLO [36] | NLO |
| Diboson | Sherpa 2.2.2 [32] | NNPDF30NNLO | NNLO |
| Triboson | Sherpa 2.2.2 | NNPDF30NNLO | NNLO |
| $V$ + jets | Sherpa 2.2.1 [32] | NNPDF30NNLO | NNLO |
| Single–top | Powheg+Pythia8.230 | NNPDF30NLO | NLO |
| $t\bar{t}$ | Powheg+Pythia8.230 | NNPDF30NLO | NLO |

Table 2: Preselection and Signal Region selection for the four categories. “OS” stands for opposite-sign, “SS” for same-sign and “ID” for identification.

| Selection | $WH, H \to \tau_{lep}\tau_{had}$ | $WH, H \to \tau_{had}\tau_{had}$ | $ZH, H \to \tau_{lep}\tau_{had}$ | $ZH, H \to \tau_{had}\tau_{had}$ |
|---|---|---|---|---|
| Preselection | exactly 1 $\tau_{had\text{-}vis}$<br>exactly 2 $\ell$<br>$b$-jet veto | exactly 2 $\tau_{had\text{-}vis}$<br>exactly 1 $\ell$<br>$b$-jet veto | exactly 1 $\tau_{had\text{-}vis}$<br>exactly 3 $\ell$<br>same-flavour, OS $\ell$ pair<br>$m_{\ell\ell} \in [81, 101]$ GeV | exactly 2 $\tau_{had\text{-}vis}$<br>exactly 2 $\ell$<br>same-flavour, OS $\ell$ pair<br>$m_{\ell\ell} \in [71, 111]$ GeV |
| Signal Region | 1 $\tau_{had\text{-}vis}$ and 1 $\tau_{lep}$ OS<br>exactly 2 $\ell$ SS<br>$\sum_{\ell} p_T(\ell) + p_T(\tau_{had\text{-}vis}) > 90$ GeV<br>$m_{ee} \notin [80, 100]$ GeV | exactly 2 $\tau_{had\text{-}vis}$ OS<br>$0.8 < \Delta R(\tau_{had\text{-}vis}, \tau_{had\text{-}vis}) < 2.8$<br>$\sum_{\tau_{had\text{-}vis}} p_T(\tau_{had\text{-}vis}) > 100$ GeV<br>$m_T(\ell, E_T^{miss}) > 20$ GeV | exactly 1 $\tau_{had\text{-}vis}$ and 1 $\tau_{lep}$ OS<br>$\sum_{\tau_{had\text{-}vis}, \tau_{lep}} p_T(\tau) > 60$ GeV | exactly 2 $\tau_{had\text{-}vis}$ OS<br>$\sum_{\tau_{had\text{-}vis}} p_T(\tau) > 75$ GeV |
| Higgs boson mass window cut (only applied in the NN-based analysis) | $m_{2T} \in [60, 130]$ GeV | $m_{2T} \in [80, 130]$ GeV | $m_{MMC} \in [100, 170]$ GeV | $m_{MMC} \in [100, 180]$ GeV |

# VH

| Category | Region | Cuts | Major process contributing to the background from misidentified jets |
|---|---|---|---|
| $WH,\ H \to \tau_{\text{had}}\tau_{\text{had}}$ | $W$+jets | PRESELECTION<br>same-sign $\tau_{\text{had-vis}}$<br>$m_{\text{T}}(\ell, E_{\text{T}}^{\text{miss}}) < 60$ GeV | $W$+jets $\sim 70\%$ |
| | $Z \to \tau\tau$ | PRESELECTION<br>$m_{2\text{T}} < 60$ GeV<br>$m_{\text{T}}(\ell, E_{\text{T}}^{\text{miss}}) < 40$ GeV | $Z \to \tau\tau \sim 50\%$ |
| | top-quark | PRESELECTION<br># $b$ jets $> 0$ | $t\bar{t} \sim 70\%$ |
| $WH,\ H \to \tau_{\text{lep}}\tau_{\text{had}}$ | $Z \to \tau\tau$ | PRESELECTION<br>opposite-sign light leptons<br>$m_{\text{coll}}(\ell, \ell) \in [60, 120]$ GeV<br>$m_{ee} \notin [80, 100]$ GeV | $Z \to \tau\tau \sim 40\%$ |
| | All Same Sign | PRESELECTION<br>all objects with same-sign<br>$m_{ee} \notin [80, 100]$ GeV | $W$+jets $\sim 70\%$ |

Table 4: Input variables for the neural networks included in all channels, and then for the specific category. The indexes "1" and "2" refer to the leading and sub-leading objects, respectively (following a $p_{\mathrm{T}}$ ordering). The symbol $\ell_\tau$ refers to the light lepton originating from a $\tau$-lepton decay, while $\ell$ (without any index) refers to a light lepton associated with the $V$ boson decay.

| All categories | $ZH,\ H\to\tau_{\mathrm{had}}\tau_{\mathrm{had}}$ | $ZH,\ H\to\tau_{\mathrm{lep}}\tau_{\mathrm{had}}$ | $WH,\ H\to\tau_{\mathrm{had}}\tau_{\mathrm{had}}$ |
|---|---|---|---|
| N-prongs($\tau_1$) | N-prongs($\tau_2$) | $p_{\mathrm{T}}(\ell_2)$ | N-prongs($\tau_2$) |
| $p_{\mathrm{T}}(\tau_1)$ | $p_{\mathrm{T}}(\tau_2)$ | $\eta(\ell_2)$ | $p_{\mathrm{T}}(\tau_2)$ |
| $\eta(\tau_1)$ | $\eta(\tau_2)$ | $\phi(\ell_2)$ | $\eta(\tau_2)$ |
| $\phi(\tau_1)$ | $\phi(\tau_2)$ | $p_{\mathrm{T}}(H)$ | $\phi(\tau_2)$ |
| $\Delta R(\tau_1,\ell_1)$ | $p_{\mathrm{T}}(\ell_2)$ | $\eta(\ell_\tau)$ | $\sqrt{\eta(\ell_1)^2+\phi(\ell_1)^2}$ |
| $p_{\mathrm{T}}(l_1)$ | $\eta(\ell_2)$ | $\phi(\ell_\tau)$ | |
| $\eta(\ell_1)$ | $\phi(\ell_2)$ | $\Delta R(\ell,\ell)$ | |
| $\phi(\ell_1)$ | $m_{\ell\ell}$ | $m_{\ell\ell}$ | |
| $p_{\mathrm{T}}(E_{\mathrm{T}}^{\mathrm{miss}})$ | $\Delta R(\ell,\ell)$ | | |
| $\phi(E_{\mathrm{T}}^{\mathrm{miss}})$ | | | |
| | $WH,\ W\to e\nu_e,\ H\to\tau_e\tau_{\mathrm{had}}$ | $WH,\ W\to e(\mu)\nu_{e(\mu)},\ H\to\tau_{\mu(e)}\tau_{\mathrm{had}}$ | $WH,\ W\to\mu\nu_\mu,\ H\to\tau_\mu\tau_{\mathrm{had}}$ |
| | $p_{\mathrm{T}}(\ell_\tau)$ | $p_{\mathrm{T}}(\ell_\tau)$ | $p_{\mathrm{T}}(\ell_\tau)$ |
| | $\eta(\ell_\tau)$ | $\eta(\ell_\tau)$ | $\eta(\ell_\tau)$ |
| | $\phi(\ell_\tau)$ | $\phi(\ell_\tau)$ | $\phi(\ell_\tau)$ |
| | $\Delta\eta(\ell,\ell_\tau)$ | $\Delta\eta(\ell,\ell_\tau)$ | $\Delta\eta(\ell,\ell_\tau)$ |
| | jet width($\tau_1$) | jet width($\tau_1$) | jet width($\tau_1$) |
| | $p_{\mathrm{T}}(H)$ | $m(\tau_1,\ell_\tau)$ | $\Delta R(\ell,\ell_\tau)$ |
| | $m(\tau_1,\ell_\tau)$ | $\Delta R(\ell,\ell_\tau)$ | $m(\tau_1,l_\tau)$ |
| | $\Delta\eta(\tau_1,\ell_\tau)$ | $\Delta\eta(\tau_1,\ell_\tau)$ | $\Delta\eta(\tau_1,\ell_\tau)$ |
| | $\Delta\phi(l_1,\ell_\tau)$ | $\sum p_{\mathrm{T}}$(all visible) | $\Delta R(\tau_1,\ell_\tau)$ |
| | $\Delta_\phi(\tau_1,\ E_{\mathrm{T}}^{\mathrm{miss}})$ | $\Delta\phi(\tau_1,E_{\mathrm{T}}^{\mathrm{miss}})$ | $\sum p_{\mathrm{T}}$(all visible) |
| | $\Delta R(\ell,\ell_\tau)$ | | $\Delta\phi(\ell_1,\ell_\tau)$ |

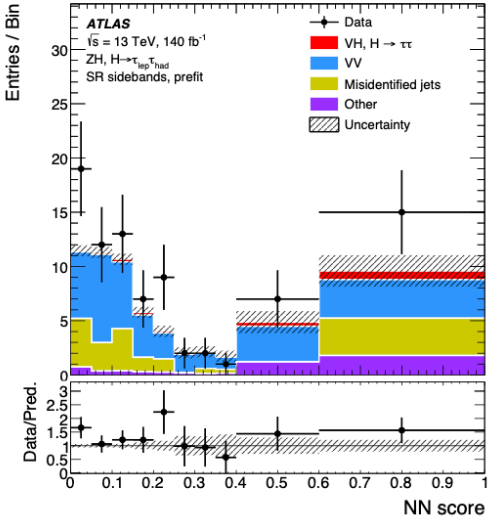
ATLAS
√s = 13 TeV, 140 fb⁻¹
ZH, H→τlepτhad
SR sidebands, prefit
Data
VH, H → ττ
VV
Misidentified jets
Other
Uncertainty
Entries / Bin
Data/Pred.
NN score

(a)

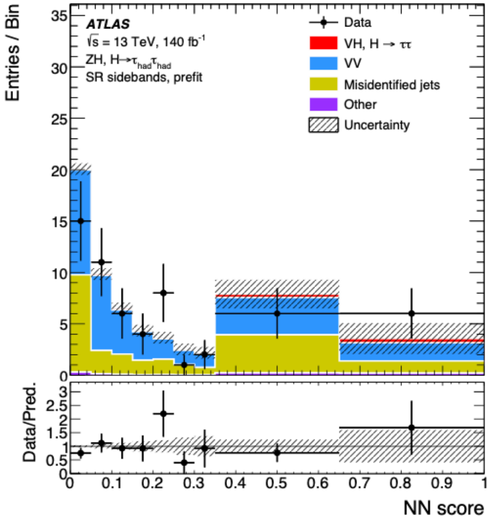
ATLAS
√s = 13 TeV, 140 fb⁻¹
ZH, H→τhadτhad
SR sidebands, prefit
Data
VH, H → ττ
VV
Misidentified jets
Other
Uncertainty
Entries / Bin
Data/Pred.
NN score

(b)

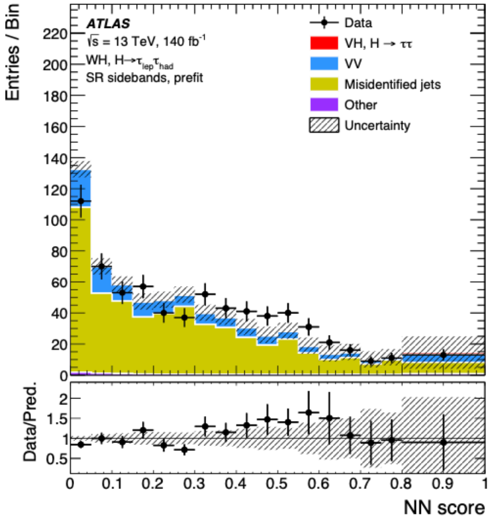
ATLAS
√s = 13 TeV, 140 fb⁻¹
WH, H→τlepτhad
SR sidebands, prefit
Data
VH, H → ττ
VV
Misidentified jets
Other
Uncertainty
Entries / Bin
Data/Pred.
NN score

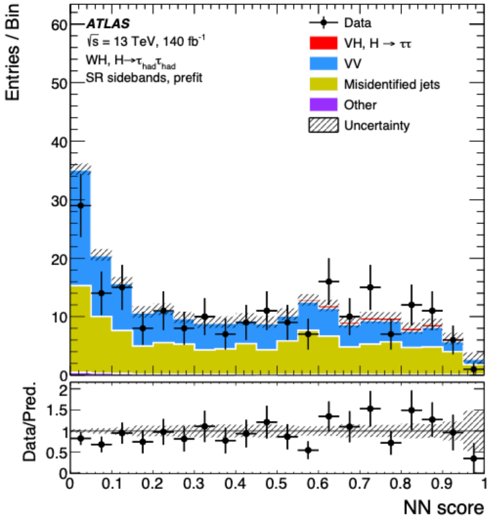
ATLAS
√s = 13 TeV, 140 fb⁻¹
WH, H→τhadτhad
SR sidebands, prefit
Data
VH, H → ττ
VV
Misidentified jets
Other
Uncertainty
Entries / Bin
Data/Pred.
NN score

# VH

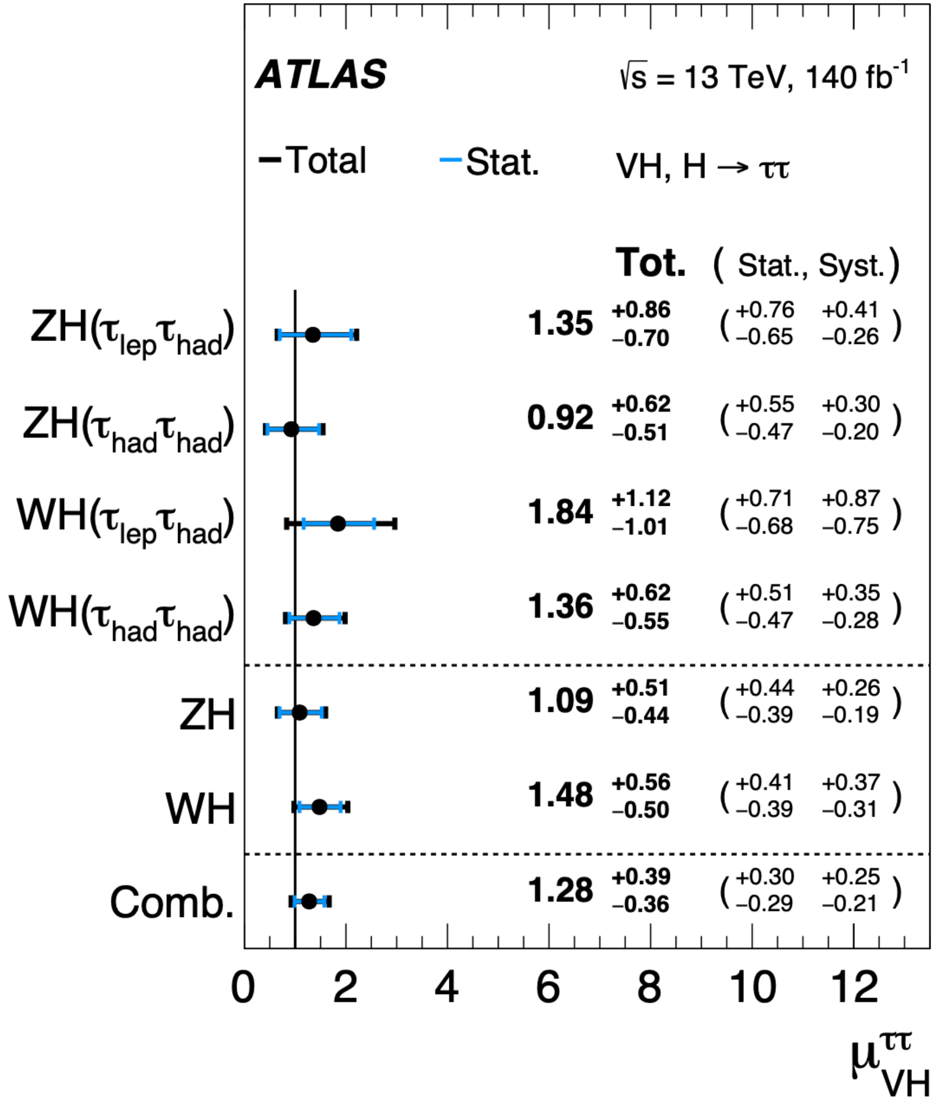

ATLAS
√s = 13 TeV, 140 fb⁻¹
Total
Stat.
VH, H → ττ
Tot. ( Stat., Syst. )
ZH(τlepτhad) 1.35 +0.86 −0.70 ( +0.76 −0.65 +0.41 −0.26 )
ZH(τhadτhad) 0.92 +0.62 −0.51 ( +0.55 −0.47 +0.30 −0.20 )
WH(τlepτhad) 1.84 +1.12 −1.01 ( +0.71 −0.68 +0.87 −0.75 )
WH(τhadτhad) 1.36 +0.62 −0.55 ( +0.51 −0.47 +0.35 −0.28 )
ZH 1.09 +0.51 −0.44 ( +0.44 −0.39 +0.26 −0.19 )
WH 1.48 +0.56 −0.50 ( +0.41 −0.39 +0.37 −0.31 )
Comb. 1.28 +0.39 −0.36 ( +0.30 −0.29 +0.25 −0.21 )
0 2 4 6 8 10 12
μ^ττ_VH

# Decay CP

# Decay CP - CP mixing

**Sakharov Conditions**

- 1- Baryon Number violation
- 2- CP violation
- 3- Thermal inequilibrium

**CP-mixed signal sample**

- Generate events without polarization POWHEG+PYTHIA8
- Use TAUSPINNER to reweight the generated events to CP-mix scenarios

# Decay CP - Decay Mode Reconstruction

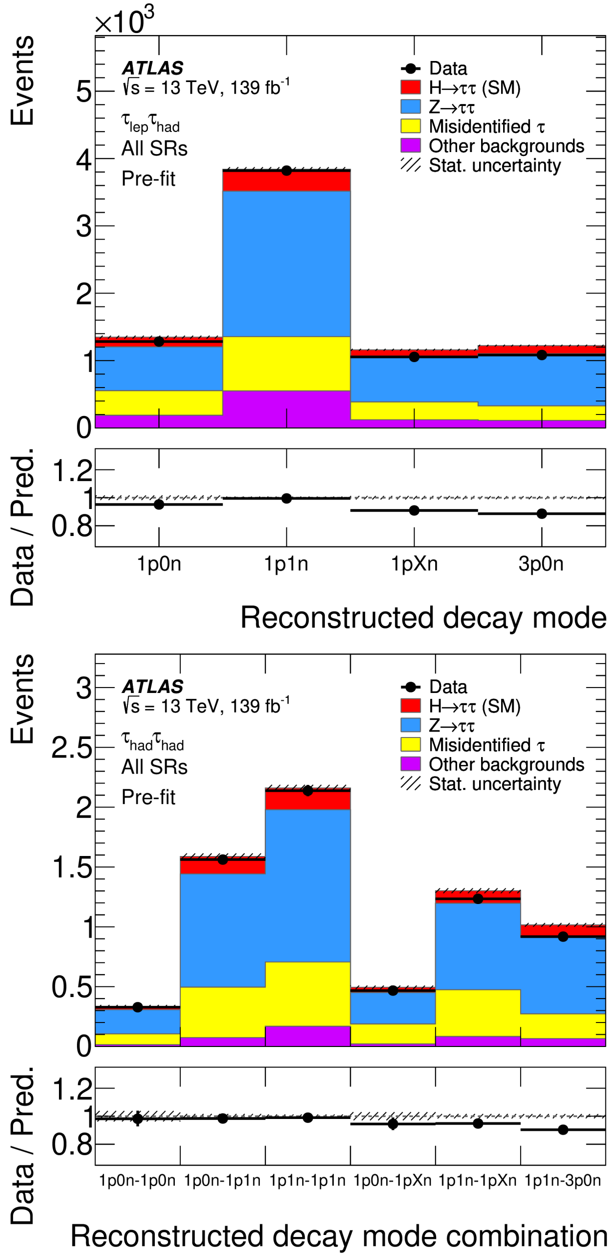


- **Ability to distinguish between single-$\pi^0$ and multi-$\pi^0$ clusters**
- **"Particle Flow" reconstruction algorithm**
  - **Determine 4-momenta of charged and neutral tau decays**
  - **Combine tracking detector and calorimeter information**
- **Decay mode classification by counting charged/neutral pions, exploit kinematic t-decay properties**
- **Use BDTs (1p0n vs. 1p1n) (1p1n vs. 1pXn)(3p0n vs. 3pXn) to improve neutral pion detection**

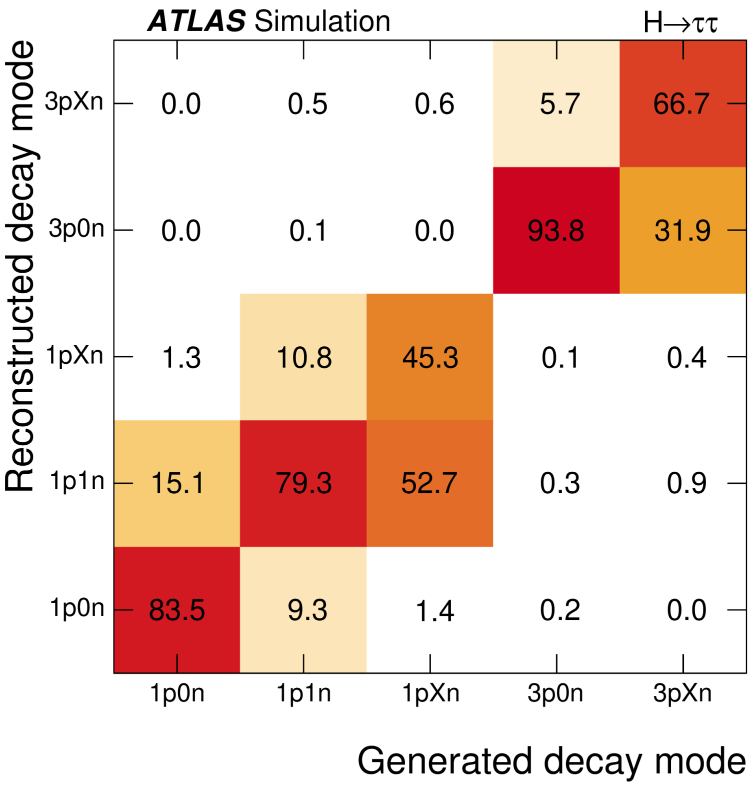


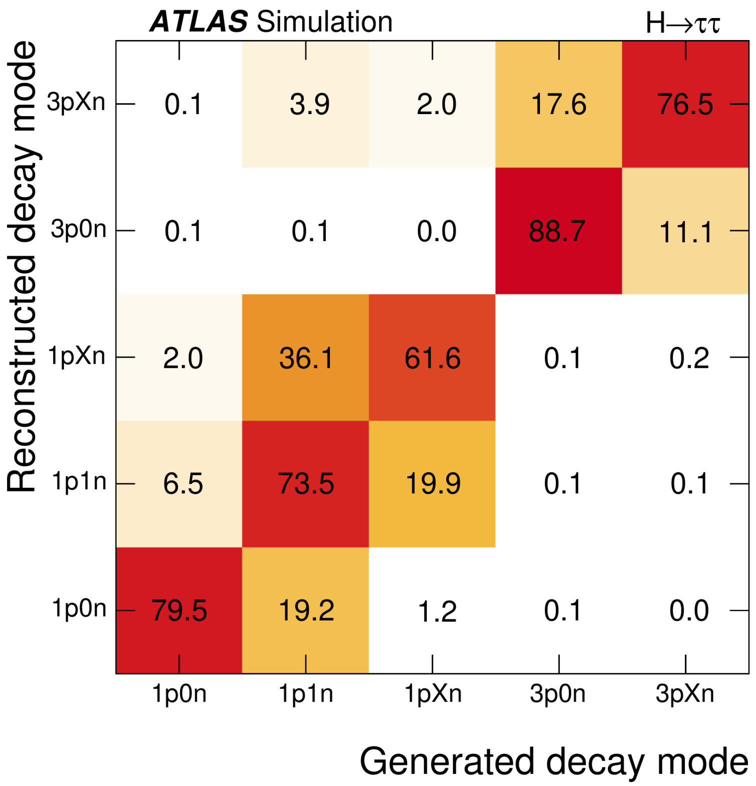

# Decay CP - Decay Plane Reconstruction

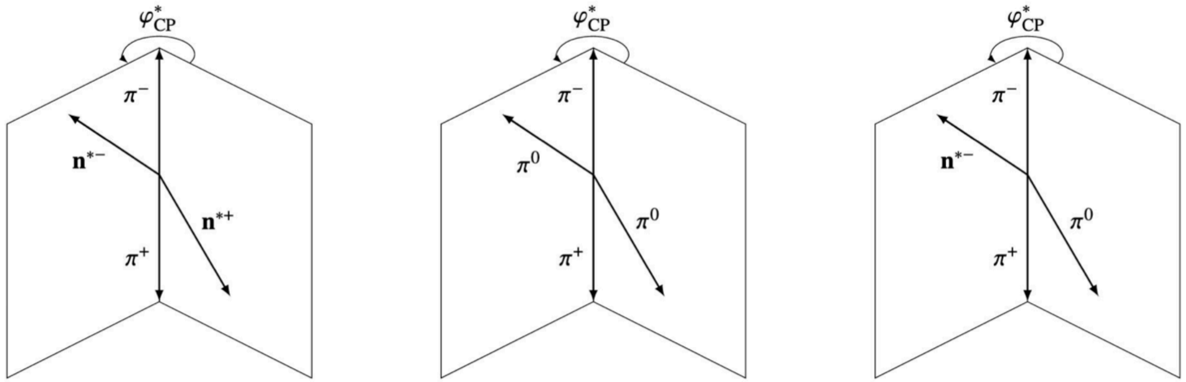


(a) Impact parameter (IP) method

(b) $\rho$-decay plane method

(c) Combined IP and $\rho$ method

$$\varphi^* = \arccos(\hat{\mathbf{n}}^{*+}_{\perp} \cdot \hat{\mathbf{n}}^{*-}_{\perp}),$$

$$\mathcal{O}^*_{CP} = \hat{\mathbf{q}}^*_{-} \cdot (\hat{\mathbf{n}}^{*+}_{\perp} \times \hat{\mathbf{n}}^{*-}_{\perp}),$$

$$\varphi^*_{CP} = \begin{cases} \varphi^* & \text{if } \mathcal{O}^*_{CP} \geq 0, \\ 2\pi - \varphi^* & \text{if } \mathcal{O}^*_{CP} < 0, \end{cases}$$

$$\varphi^* = \arccos(\hat{\mathbf{q}}^{*0+}_{\perp} \cdot \hat{\mathbf{q}}^{*0-}_{\perp}),$$

$$O^*_{\mathrm{CP}} = \hat{\mathbf{q}}^{*-} \cdot (\hat{\mathbf{q}}^{*0+}_{\perp} \times \hat{\mathbf{q}}^{*0-}_{\perp}).$$

$$\varphi^{*\prime} = \begin{cases} \varphi^* & \text{if } O^*_{\mathrm{CP}} \geq 0 \\ 2\pi - \varphi^* & \text{if } O^*_{\mathrm{CP}} < 0. \end{cases}$$

$$y_- = \frac{E_{\pi^-} - E_{\pi^0}}{E_{\pi^-} + E_{\pi^0}}, \quad y_+ = \frac{E_{\pi^+} - E_{\pi^0}}{E_{\pi^+} + E_{\pi^0}},$$

$$\varphi^*_{\mathrm{CP}} = \begin{cases} \varphi^{*\prime} & \text{if } y_+ y_- \geq 0 \\ \varphi^{*\prime} + \pi & \text{if } y_+ y_- < 0. \end{cases}$$

$$\varphi^* = \arccos(\hat{\mathbf{q}}^{*0+}_{\perp} \cdot \hat{\mathbf{n}}^{*-}_{\perp}),$$

$$O^*_{\mathrm{CP}} = \hat{\mathbf{q}}^{*-} \cdot (\hat{\mathbf{q}}^{*+}_{\perp} \times \hat{\mathbf{n}}^{*-}_{\perp}),$$

$$\varphi^{*\prime} = \begin{cases} \varphi^{*\prime} & \text{if } O^*_{CP} \geq 0 \\ 2\pi - \varphi^{*\prime} & \text{if } O^*_{CP} < 0. \end{cases}$$

$$y_+ = \frac{E_{\pi^+} - E_{\pi^0}}{E_{\pi^+} + E_{\pi^0}},$$

$$\varphi^*_{\mathrm{CP}} = \begin{cases} \varphi^{*\prime} & \text{if } y_+ \geq 0 \\ \varphi^{*\prime} + \pi & \text{if } y_+ < 0. \end{cases}$$

- **IP method (for $l$ = e, μ and 1p0n)**
  - Charged pion ($\pi^{\pm}$) and impact parameter ($\mathbf{n}^{*\pm}$)
- **ρ decay plane method (1p1n, 1pXn)**
  - Charged pion and neutral pion ($\pi^0$)
- **Combined**
  - Combination of methods w.r.t. decay modes
- **$a_1$ decay method (3p0n)**
  - Modified ρ method or 3-prong decays

| Notation | Decay mode | Branching fraction |
|---|---|---|
| $\ell$ | $\ell^{\pm}\bar{\nu}\nu$ | 35.2% |
| 1p0n | $h^{\pm}\nu$ ($\pi^{\pm}\nu$) | 11.5% (10.8%) |
| 1p1n | $h^{\pm}\pi^0\nu$ ($\pi^{\pm}\pi^0\nu$) | 25.9% (25.5%) |
| 1pXn | $h^{\pm} \geq 2\pi^0\nu$ ($\pi^{\pm}2\pi^0\nu$) | 10.8% (9.3%) |
| 3p0n | $3h^{\pm}\nu$ ($3\pi^{\pm}\nu$) | 9.8% (9.0%) |

| Decay channel | Decay mode combination | Method | Fraction in all $\tau$-lepton-pair decays |
|---|---|---|---|
| $\tau_{\mathrm{lep}}\tau_{\mathrm{had}}$ | $\ell$–1p0n | IP | 8.1% |
| | $\ell$–1p1n | IP–$\rho$ | 18.3% |
| | $\ell$–1pXn | IP–$\rho$ | 7.6% |
| | $\ell$–3p0n | IP–$a_1$ | 6.9% |
| $\tau_{\mathrm{had}}\tau_{\mathrm{had}}$ | 1p0n–1p0n | IP | 1.3% |
| | 1p0n–1p1n | IP–$\rho$ | 6.0% |
| | 1p1n–1p1n | $\rho$ | 6.7% |
| | 1p0n–1pXn | IP–$\rho$ | 2.5% |
| | 1p1n–1pXn | $\rho$ | 5.6% |
| | 1p1n–3p0n | $\rho$–$a_1$ | 5.1% |

# Decay CP - Preselection



| Preselection: $\tau_{lep}\tau_{had}$ channel |
|---|
| Leading jet with $p_T > 40$ GeV |
| One lepton (e or $\mu$) as $\tau_{lep}$ candidate |
| One $\tau_{had}$ candidate, classified as 1p0n, 1p1n, 1pXn and 3p0n |
| Opposite electric charge between $\tau_{lep}$ and $\tau_{had}$ candidates |
| $p_T\ (\tau_{lep}) > 21$ to $27.3$ GeV, $p_T\ (\tau_{had}) > 30$ GeV |
| $\Delta R_{\tau\tau} < 2.5$, $\lvert\Delta\eta_{\tau\tau}\rvert < 1.5$ |
| Collinear approx.: $0.1 < x_1 < 1.4$, $0.1 < x_2 < 1.2$ |
| $E_T^{miss} > 20$ GeV |
| $m_T < 70$ GeV |

| Preselection: $\tau_{had}\tau_{had}$ channel |
|---|
| Leading jet with $p_T > 70$ GeV, $\lvert\eta\rvert < 3.2$ |
| Two $\tau_{had}$ candidates, classified as 1p0n, 1p1n, 1pXn and 3p0n |
| Opposite electric charge between two $\tau_{had}$ candidates |
| No electron or muon |
| $p_T(\tau_1) > 40$ GeV, $p_T(\tau_2) > 30$ GeV |
| $0.6 < \Delta R_{\tau\tau} < 2.5$, $\lvert\Delta\eta_{\tau\tau}\rvert < 1.5$ |
| Collinear approx.: $0.1 < x_1 < 1.4$, $0.1 < x_2 < 1.4$ |
| $E_T^{miss} > 20$ GeV |

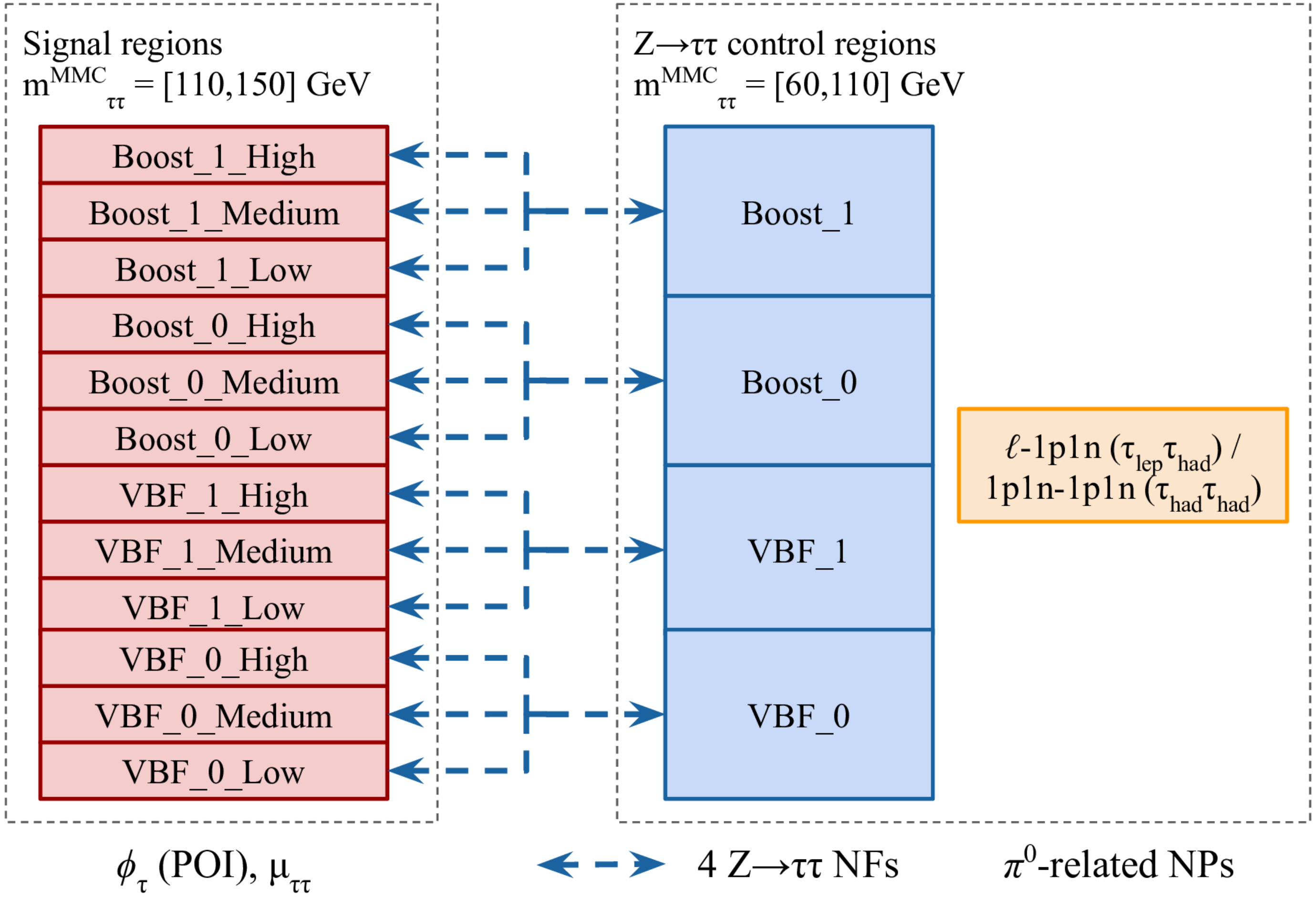


| VBF | | Boost | |
|---|---|---|---|
| $p_T^{j_2} > 30$ GeV<br>$m_{jj} > 400$ GeV<br>$\lvert\Delta\eta_{jj}\rvert > 3.0$<br>$\eta_{j_1} \cdot \eta_{j_2} < 0$<br>Central $\tau$-leptons | | Not VBF<br>$p_T^{\tau\tau} > 100$ GeV | |
| Signal region ($110 < m^{MMC}_{\tau\tau} < 150$ GeV) | | | |
| VBF_1 | VBF_0 | Boost_1 | Boost_0 |
| BDT(VBF) > 0 | BDT(VBF) < 0 | $\Delta R_{\tau\tau} < 1.5$ and<br>$p_T^{\tau\tau} > 140$ GeV | $\Delta R_{\tau\tau} > 1.5$ or<br>$p_T^{\tau\tau} < 140$ GeV |
| $Z \rightarrow \tau\tau$ control region ($60 < m^{MMC}_{\tau\tau} < 110$ GeV) | | | |
| VBF_1 Z CR | VBF_0 Z CR | Boost_1 Z CR | Boost_0 Z CR |

# Decay CP - Optimized SR Selection

| Channel | Signal region | Decay mode combination | Selection criteria |
| --- | --- | --- | --- |
| $\tau_{\text{lep}}\tau_{\text{had}}$ | High | $\ell$–1p0n | $\lvert d_0^{\text{sig}}(e)\rvert > 2.5$ or $\lvert d_0^{\text{sig}}(\mu)\rvert > 2.0$<br>$\lvert d_0^{\text{sig}}(\tau_{1\text{p0n}})\rvert > 1.5$ |
| | | $\ell$–1p1n | $\lvert d_0^{\text{sig}}(e)\rvert > 2.5$ or $\lvert d_0^{\text{sig}}(\mu)\rvert > 2.0$<br>$\lvert y^{\rho}(\tau_{1\text{p1n}})\rvert > 0.1$ |
| | Medium | $\ell$–1pXn | $\lvert d_0^{\text{sig}}(e)\rvert > 2.5$ or $\lvert d_0^{\text{sig}}(\mu)\rvert > 2.0$<br>$\lvert y^{\rho}(\tau_{1\text{pXn}})\rvert > 0.1$ |
| | | $\ell$–3p0n | $\lvert d_0^{\text{sig}}(e)\rvert > 2.5$ or $\lvert d_0^{\text{sig}}(\mu)\rvert > 2.0$<br>$\lvert y^{a_1}(\tau_{3\text{p0n}})\rvert > 0.6$ |
| | Low | All above | Not satisfying selection criteria |

| Channel | Signal region | Decay mode combination | Selection criteria |
| --- | --- | --- | --- |
| $\tau_{\text{had}}\tau_{\text{had}}$ | High | 1p0n–1p0n | $\lvert d_0^{\text{sig}}(\tau_1)\rvert > 1.5$<br>$\lvert d_0^{\text{sig}}(\tau_2)\rvert > 1.5$ |
| | | 1p0n–1p1n | $\lvert d_0^{\text{sig}}(\tau_{1\text{p0n}})\rvert > 1.5$<br>$\lvert y^{\rho}(\tau_{1\text{p1n}})\rvert > 0.1$ |
| | | 1p1n–1p1n | $\lvert y^{\rho}(\tau_1)y^{\rho}(\tau_2)\rvert > 0.2$ |
| | Medium | 1p0n–1pXn | $\lvert d_0^{\text{sig}}(\tau_{1\text{p0n}})\rvert > 1.5$<br>$\lvert y^{\rho}(\tau_{1\text{pXn}})\rvert > 0.1$ |
| | | 1p1n–1pXn | $\lvert y^{\rho}(\tau_{1\text{p1n}})y^{\rho}(\tau_{1\text{pXn}})\rvert > 0.2$ |
| | | 1p1n–3p0n | $\lvert y^{\rho}(\tau_{1\text{p1n}})\rvert > 0.1$<br>$\lvert y^{a_1}(\tau_{3\text{p0n}})\rvert > 0.6$ |
| | Low | All above | Not satisfying selection criteria |

# Decay CP - SR Distributions

Eur. Phys. J. C 83, 563 (2023)

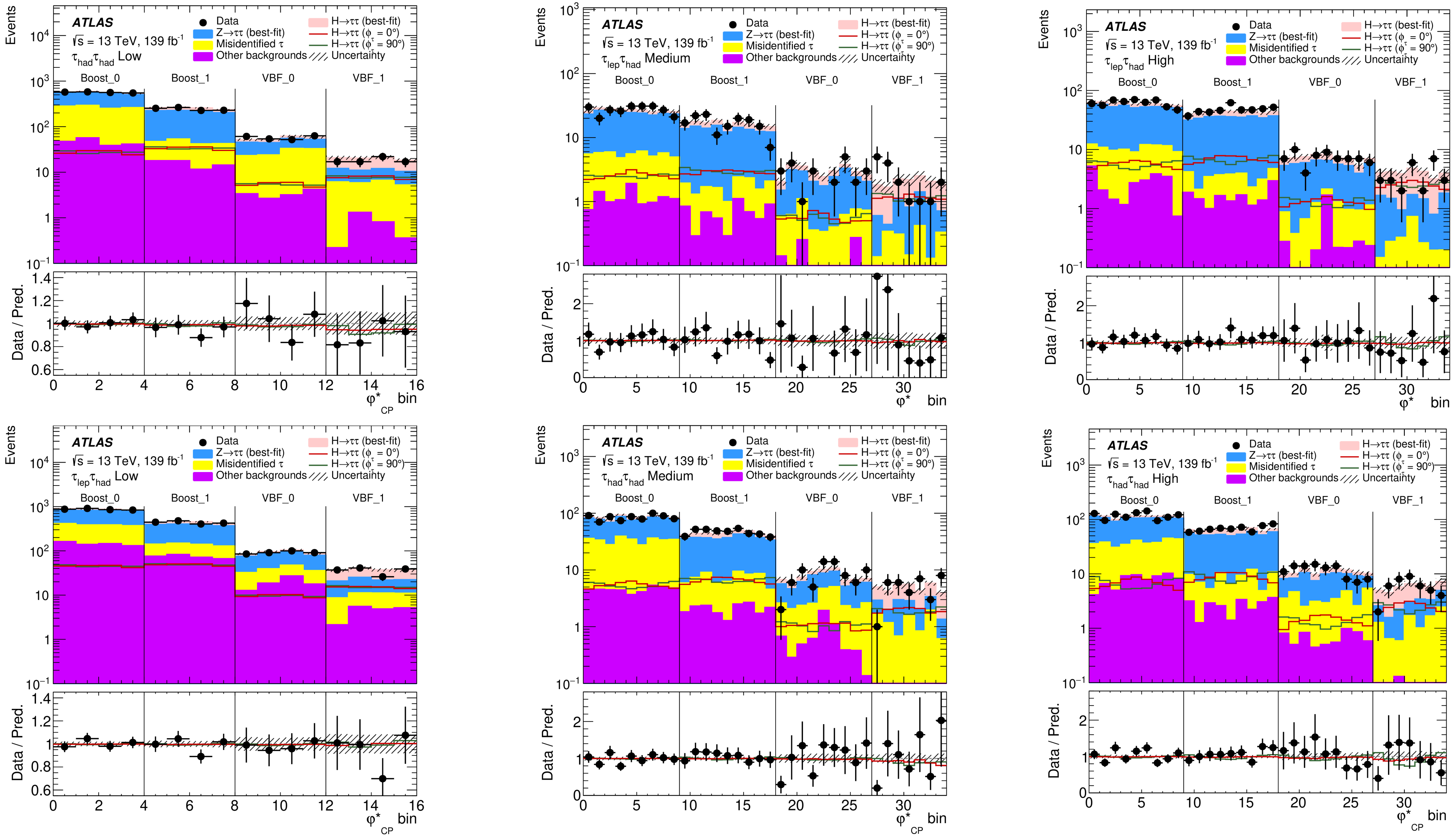

# Decay CP - CR Distributions

Angular res. & energy scale of PI0 affects phi shape for 1p1n,1pXn

Overestimated priors -> impact too large -> constrain with ZCR

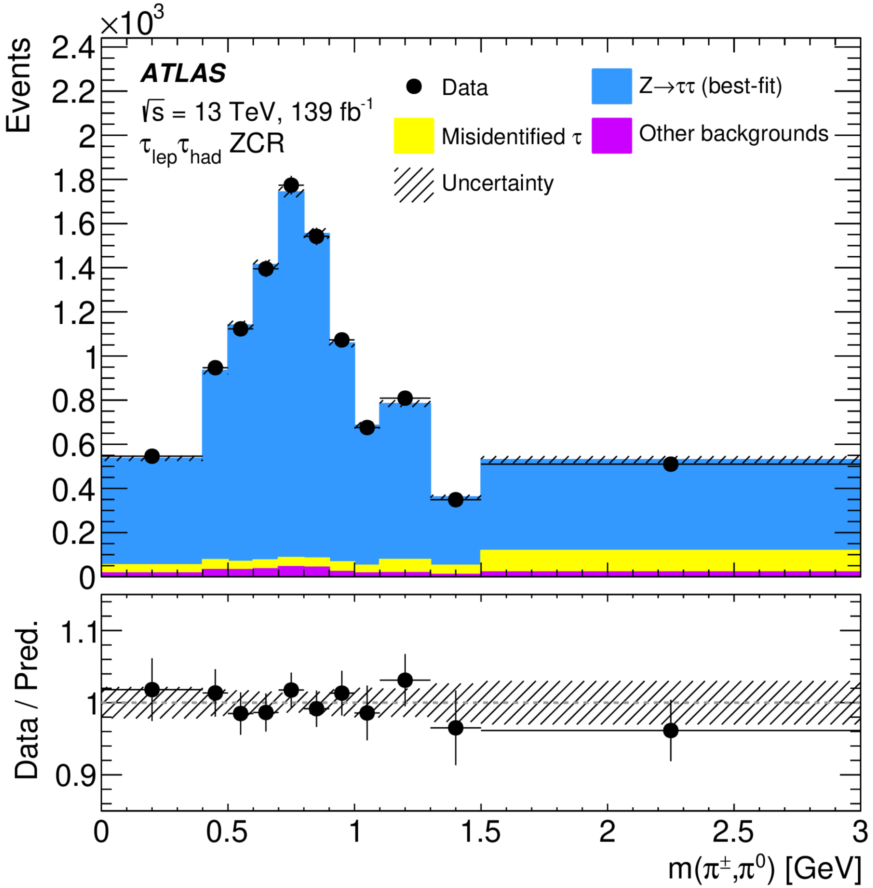


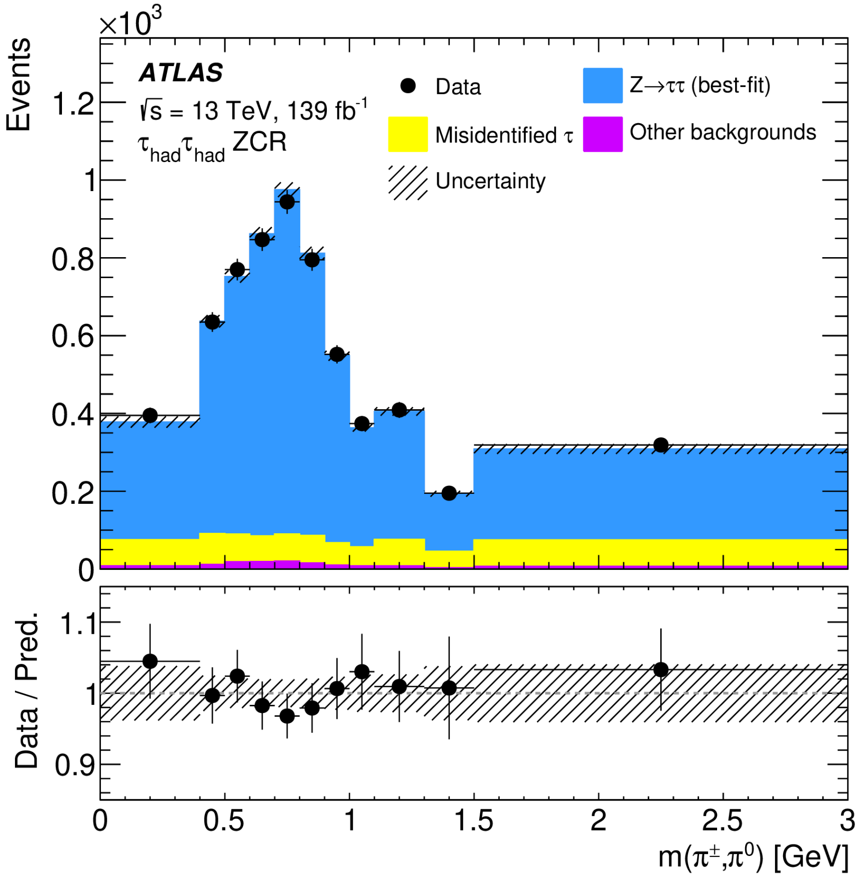


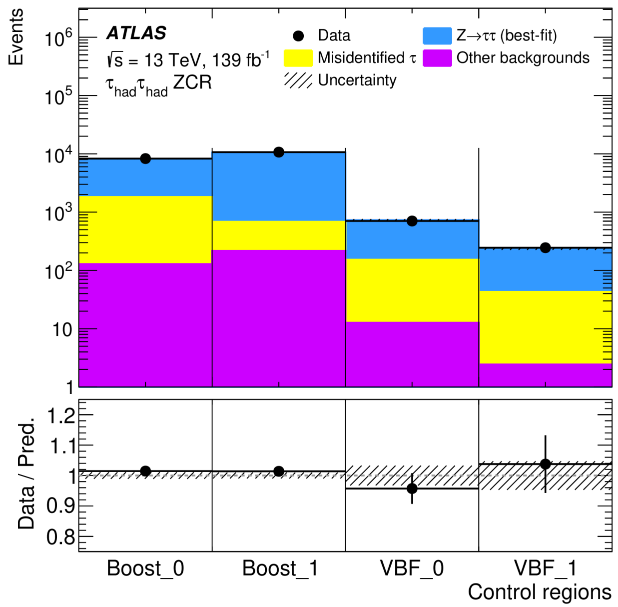


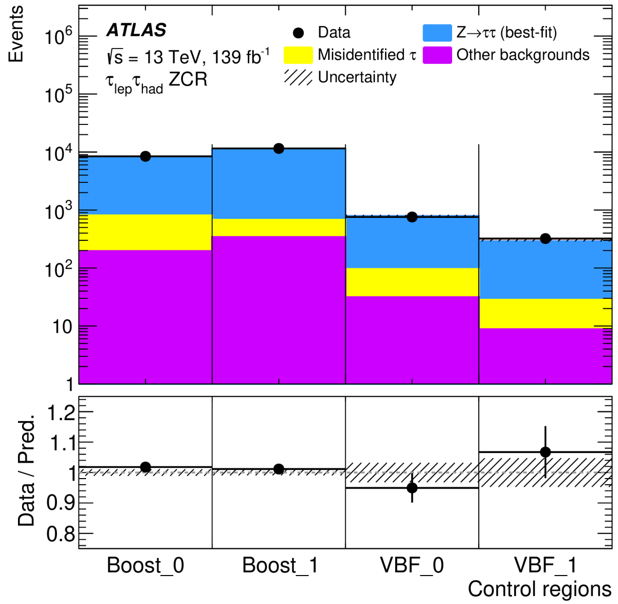

# Decay CP - Fit Results

| Fitted parameters | Observed | Expected |
|---|---|---|
| $\phi_\tau$ | $9^\circ \pm 16^\circ$ | $0^\circ \pm 28^\circ$ |
| $\mu_{\tau\tau}$ | $1.02^{+0.20}_{-0.20}$ | $1.00^{+0.21}_{-0.21}$ |
| $NF^{Boost\_1}_{Z\to\tau\tau}$ | $1.01 \pm 0.05$ | $1.00 \pm 0.04$ |
| $NF^{Boost\_0}_{Z\to\tau\tau}$ | $1.02 \pm 0.05$ | $1.00 \pm 0.05$ |
| $NF^{VBF\_1}_{Z\to\tau\tau}$ | $1.04 \pm 0.08$ | $1.00 \pm 0.08$ |
| $NF^{VBF\_0}_{Z\to\tau\tau}$ | $0.95 \pm 0.07$ | $1.00 \pm 0.08$ |

| Set of nuisance parameters | Impact on $\phi_\tau$ [degrees] |
|---|---|
| Jet energy scale | 3.4 |
| Jet energy resolution | 2.5 |
| Pile-up jet tagging | 0.5 |
| Jet flavour tagging | 0.2 |
| $E_T^{miss}$ | 0.4 |
| Electron | 0.3 |
| Muon | 0.9 |
| $\tau_{had}$ reconstruction | 1.0 |
| Misidentified $\tau$ | 0.6 |
| $\tau_{had}$ decay mode classification | 0.3 |
| $\pi^0$ angular resolution and energy scale | 0.2 |
| Track ($\pi^\pm$, impact parameter) | 0.7 |
| Luminosity | 0.1 |
| Theory uncertainty in $H \to \tau\tau$ processes | 1.5 |
| Theory uncertainty in $Z \to \tau\tau$ processes | 1.1 |
| Simulated background sample statistics | 1.4 |
| Signal normalisation | 1.4 |
| Background normalisation | 0.6 |
| Total systematic uncertainty | 5.2 |
| Data sample statistics | 15.6 |
| Total | 16.4 |

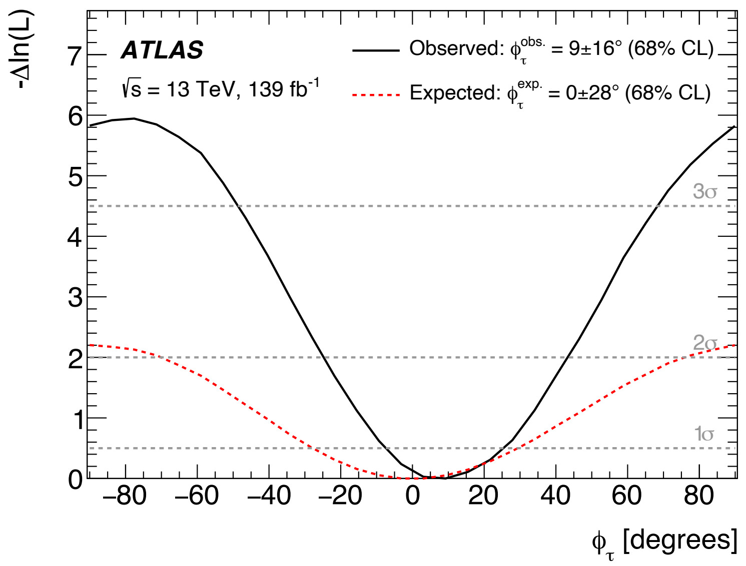
ATLAS
$\sqrt{s}$ = 13 TeV, 139 fb$^{-1}$
Observed: $\phi_\tau^{obs.}$ = 9±16° (68% CL)
Expected: $\phi_\tau^{exp.}$ = 0±28° (68% CL)
-Δln(L)
3σ
2σ
1σ
$\phi_\tau$ [degrees]

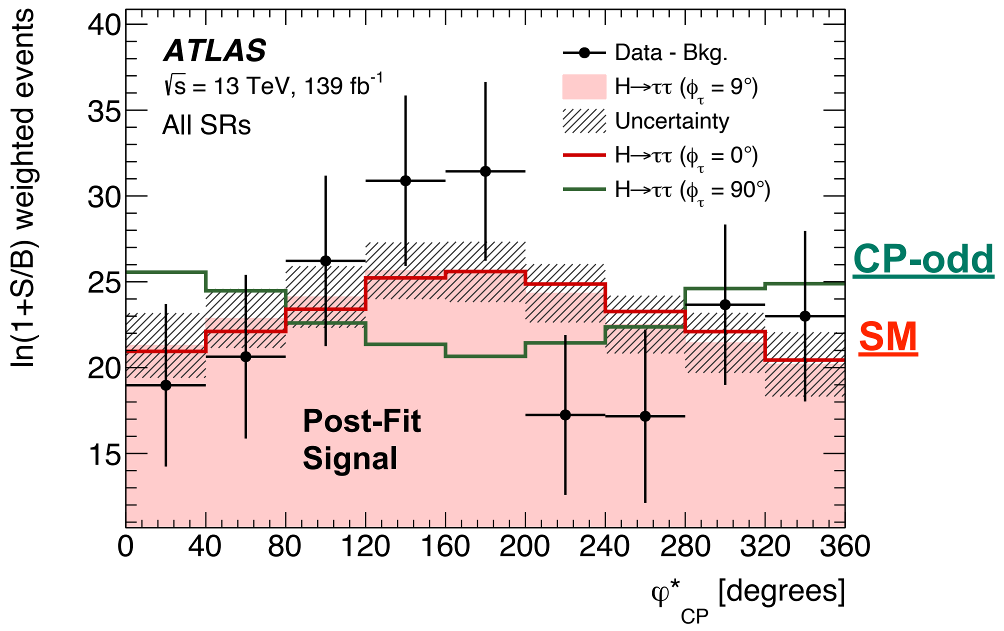
ATLAS
$\sqrt{s}$ = 13 TeV, 139 fb$^{-1}$
All SRs
Data - Bkg.
H→ττ ($\phi_\tau$ = 9°)
Uncertainty
H→ττ ($\phi_\tau$ = 0°)
H→ττ ($\phi_\tau$ = 90°)
Post-Fit Signal
ln(1+S/B) weighted events
$\varphi^*_{CP}$ [degrees]
CP-odd
SM

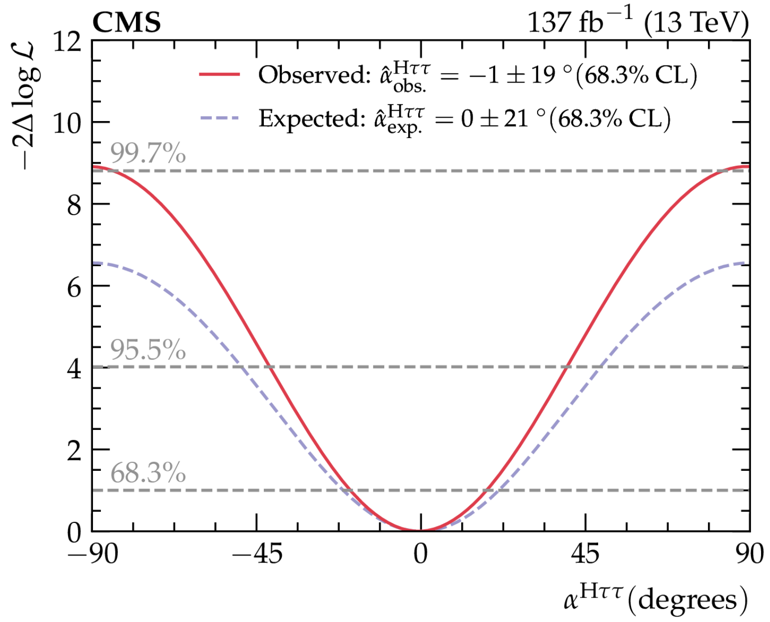
CMS
137 fb$^{-1}$ (13 TeV)
Observed: $\hat{\alpha}^{H\tau\tau}_{obs.} = -1 \pm 19$ °(68.3% CL)
Expected: $\hat{\alpha}^{H\tau\tau}_{exp.} = 0 \pm 21$ °(68.3% CL)
$-2\Delta\log\mathcal{L}$
99.7%
95.5%
68.3%
$\alpha^{H\tau\tau}$(degrees)

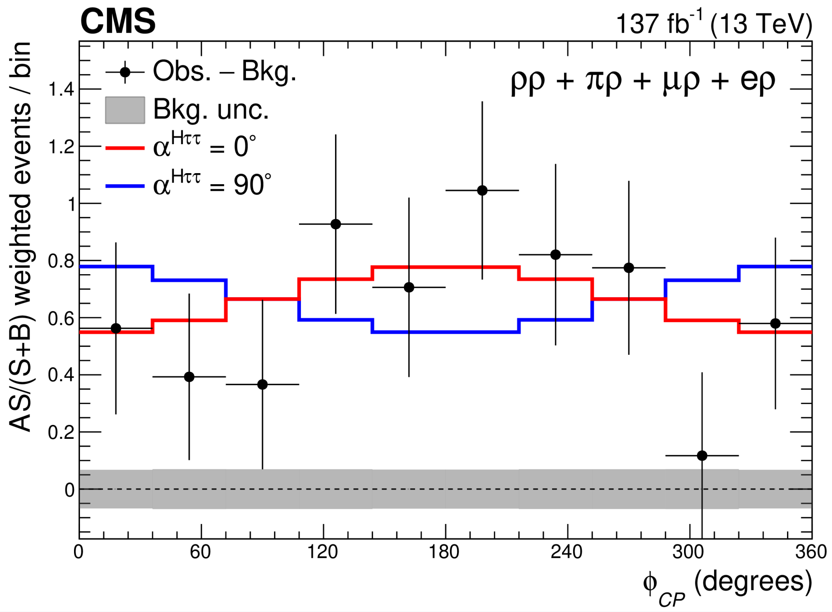
CMS
137 fb$^{-1}$ (13 TeV)
Obs. – Bkg.
Bkg. unc.
$\alpha^{H\tau\tau}$ = 0°
$\alpha^{H\tau\tau}$ = 90°
ρρ + πρ + μρ + eρ
AS/(S+B) weighted events / bin
$\phi_{CP}$ (degrees)

# LFV

# LFV - Samples and categories

| Process | Generator ME | Generator PS | PDF set ME | PDF set PS | Tune | Order |
|---|---|---|---|---|---|---|
| **Higgs boson** | | | | | | |
| $ggF$ | Powheg Box v2 | Pythia 8 | PDF4LHC15nnlo | CTEQ6L1 | AZNLO | $N^3$LO QCD + NLO EW |
| VBF | Powheg Box v2 | Pythia 8 | PDF4LHC15nlo | CTEQ6L1 | AZNLO | NNLO QCD + NLO EW |
| $VH$ | Powheg Box v2 | Pythia 8 | PDF4LHC15nlo | CTEQ6L1 | AZNLO | NNLO QCD + NLO EW |
| $t\bar{t}H$ | Powheg Box v2 | Pythia 8 | NNPDF3.0nnlo | NNPDF2.3lo | A14 | NLO QCD + NLO EW |
| **Background** | | | | | | |
| $V$ + jets (QCD/EW) | Sherpa 2.2.1 | | NNPDF3.0nnlo | | Sherpa | NNLO QCD + LO EW |
| $V$ + jets (QCD/EW)* | Powheg Box v2 | Pythia 8 | CT10nlo | CTEQ6L1 | AZNLO | NNLO |
| Diboson | Sherpa 2.2.1 | | NNPDF3.0nnlo | | Sherpa | NLO |
| $t\bar{t}$ | Powheg Box v2 | Pythia 8 | NNPDF3.0nnlo | NNPDF2.3lo | A14 | NNLO + NNLL |
| Single top | Powheg Box v2 | Pythia 8 | NNPDF3.0nnlo | NNPDF2.3lo | A14 | NLO |

| Method | Channel | Category | Region | 1 POI fit | 2 POI fit |
|---|---|---|---|---|---|
| MC-template | $\ell\tau_{\ell'}$ | *non-VBF* | SR | ✓ | ✓ |
| | | | $Z \to \tau\tau$ CR | ✓ | ✓ |
| | | | Top-quark CR | ✓ | ✓ |
| | | *VBF* | SR | | ✓ |
| | | | $Z \to \tau\tau$ CR | | ✓ |
| | | | Top-quark CR | | ✓ |
| MC-template | $\ell\tau_{\text{had}}$ | *non-VBF* | SR | ✓ | ✓ |
| | | *VBF* | SR | ✓ | ✓ |
| Symmetry | $\ell\tau_{\ell'}$ | *non-VBF* | SR | | |
| | | *VBF* | SR | ✓ | |

| Selection | $\ell\tau_{\ell'}$ | $\ell\tau_{had}$ |
|---|---|---|
| *Baseline* | exactly $1e$ and $1\mu$, OS<br>$\tau_{had}$-veto<br>–<br>$b$-veto<br>$p_T^{\ell_1} > 45$ (35) GeV MC-template (Symmetry method)<br>$p_T^{\ell_2} > 15$ GeV<br>30 GeV $< m_{\ell_1\ell_2} <$ 150 GeV<br>$0.2 < p_T^{track}(\ell_2 = e)/p_T^{cluster}(\ell_2 = e) < 1.25$ (MC-template)<br>track $d_0$ significance requirement (see text)<br>$\lvert z_0 \sin\theta\rvert < 0.5$ mm | exactly $1\ell$ and $1\tau_{had\text{-}vis}$, OS<br>$\tau_{had}$Tight ID<br>Medium eBDT ($e\tau_{had}$)<br>$b$-veto<br>$p_T^{\ell} > 27.3$ GeV<br>$p_T^{\tau_{had\text{-}vis}} > 25$ GeV, $\lvert\eta^{\tau_{had\text{-}vis}}\rvert < 2.4$<br>$\sum_{i=\ell,\tau_{had\text{-}vis}} \cos\Delta\phi(i, E_T^{miss}) > -0.35$<br>$\lvert\Delta\eta(\ell, \tau_{had\text{-}vis})\rvert < 2$ |
| *VBF* | *Baseline*<br>$\geq 2$ jets, $p_T^{j_1} > 40$ GeV, $p_T^{j_2} > 30$ GeV<br>$\lvert\Delta\eta_{jj}\rvert > 3$, $m_{jj} > 400$ GeV | |
| *non-VBF* | *Baseline* plus fail *VBF* categorisation<br>– | veto events if<br>$90 < m_{vis}(e, \tau_{had\text{-}vis}) < 100$ GeV |

| Selection | $\ell\tau_{\ell'}$ | $\ell\tau_{had}$ |
|---|---|---|
| misidentified background CR | *non-VBF* (or *VBF*) category with<br>statistically independent lepton ($\ell$ or $\tau_{had\text{-}vis}$) selection, see text | |
| $Z \to \mu\mu$ CR/VR ($\ell\tau_{\ell'}/\ell\tau_{had}$) | *Baseline* with 35 GeV $< p_T^{\ell_1} <$ 45 GeV<br>75 GeV $< m_{\ell_1\ell_2} <$ 100 GeV<br>$\lvert\Delta\phi(\ell_2, E_T^{miss})\rvert < 1.5$<br>$1.25 < p_T^{track}(\ell_2)/p_T^{cluster}(\ell_2) < 3$ | *Baseline*<br>$\lvert\eta(\tau)\rvert < 0.1$<br>90 GeV $< m_{coll}(\mu, \tau) <$ 110 GeV |
| top-quark CR | *non-VBF* (or *VBF*) selection<br>with inverted $b$-veto requirement | – |
| $Z \to \tau\tau$ CR | *non-VBF* (or *VBF*) selection<br>with 35 GeV $< p_T^{\ell_1} <$ 45 GeV | – |
| Diboson VR | *Baseline*<br>$p_T^{\ell_2} > 30$ GeV<br>100 GeV $< m_{\ell_1\ell_2} <$ 150 GeV<br>$m_T > 30$ GeV<br>veto events with jets with $p_T > 30$ GeV | – |

# LFV - MVA Inputs

| Variable | $\ell\tau_{\mathrm{had}}$ non-VBF | $\ell\tau_{\mathrm{had}}$ VBF | $\ell\tau_{\ell'}$ MC-template non-VBF | $\ell\tau_{\ell'}$ MC-template VBF | $\ell\tau_{\ell'}$ Symmetry non-VBF | $\ell\tau_{\ell'}$ Symmetry VBF |
|---|---|---|---|---|---|---|
| $m_{\mathrm{coll}}$ | ✓ | ✓ | ✓ | ✓ | ✓ | ✓ |
| $m_{\mathrm{vis}}$ | ✓ | ✓ | ✓ | ✓ | ✓ | ✓ |
| $m_{\mathrm{MMC}}$ | | | ✓ | ✓ | ✓ | ✓ |
| $m_{\mathrm{T}}(\tau, E_{\mathrm{T}}^{\mathrm{miss}})$ | ✓ | ✓ | | | ✓ | ✓ |
| $m_{\mathrm{T}}(\ell_H, E_{\mathrm{T}}^{\mathrm{miss}})$ | ✓ | ✓ | | | ✓ | ✓ |
| $m_{\mathrm{T}}(\ell_1, E_{\mathrm{T}}^{\mathrm{miss}})$ | | | ✓ | ✓ | | |
| $m_{\mathrm{T}}(\ell_2, E_{\mathrm{T}}^{\mathrm{miss}})$ | | | ✓ | ✓ | | |
| $E_{\mathrm{T}}^{\mathrm{miss}}$ | ✓ | ✓ | ✓ | ✓ | ✓ | ✓ |
| $p_{\mathrm{T}}(\ell_H)$ | ✓ | ✓ | | | | |
| $p_{\mathrm{T}}(\tau_{\text{had-vis}})$ | ✓ | ✓ | | | | |
| $p_{\mathrm{T}}(\ell_2 + E_{\mathrm{T}}^{\mathrm{miss}})/p_{\mathrm{T}}(\ell_1)$ | | | ✓ | ✓ | | |
| $p_{\mathrm{T}}^{\mathrm{rest}}(\ell_H)$ | | | ✓ | ✓ | ✓ | ✓ |
| $p_{\mathrm{T}}^{\mathrm{rest}}(\ell_\tau)$ | | | ✓ | ✓ | ✓ | ✓ |
| $p_{\mathrm{T}}^{\mathrm{tot}}$ | | | | ✓ | ✓ | ✓ |
| $p_{\mathrm{T}}(\ell_H)/E_{\mathrm{T}}^{\mathrm{miss}}$ | | | | | ✓ | ✓ |
| $p_{\mathrm{T}}(\ell_H)/p_{\mathrm{T}}(\ell_\tau)$ | | | | | ✓ | ✓ |
| $p_{\mathrm{T}}(\ell_\tau + E_{\mathrm{T}}^{\mathrm{miss}})/p_{\mathrm{T}}(\ell_H)$ | | | | | ✓ | ✓ |
| $\sum p_{\mathrm{T}}$ | | | | | ✓ | ✓ |
| $\Delta R(\ell_H, \tau)$ | ✓ | ✓ | ✓ | ✓ | ✓ | ✓ |
| $\Delta\eta(\ell_H, \tau)$ | ✓ | ✓ | | | ✓ | ✓ |
| $\Delta\phi(\ell_H, \tau)$ | ✓ | | | | ✓ | |
| $\Delta\phi(\ell_\tau, E_{\mathrm{T}}^{\mathrm{miss}})$ | | | ✓ | ✓ | ✓ | ✓ |
| $\lvert\Delta\phi(\ell_H, E_{\mathrm{T}}^{\mathrm{miss}})\rvert - \lvert\Delta\phi(\tau_{\text{had-vis}}, E_{\mathrm{T}}^{\mathrm{miss}})\rvert$ | ✓ | | | | | |
| $\Delta\alpha$ | | | ✓ | ✓ | ✓ | ✓ |
| $\Delta\Phi\,(\ell_H, E_{\mathrm{T}}^{\mathrm{miss}})$ | | ✓ | ✓ | ✓ | ✓ | ✓ |
| $\Delta d_0\,(\ell_1, \ell_2)$ | | | ✓ | ✓ | ✓ | |
| $\sigma_{d_0}^{\ell_\tau}$ | | | ✓ | ✓ | | |
| $\eta(\tau_{\text{had-vis}})$ | ✓ | ✓ | | | | |
| $m_{\mathrm{jj}}$ | | ✓ | | ✓ | | ✓ |
| $N_{\mathrm{jets}(p_{\mathrm{T}}>30\mathrm{GeV})}$ | | ✓ | | | | |
| $\lvert\Delta\eta_{\mathrm{jj}}\rvert$ | | ✓ | | | | ✓ |
| $\Delta R(\mathrm{j}, \mathrm{j})$ | | | | ✓ | | ✓ |
| $\lvert\Delta\eta_{\mathrm{jj}}\rvert \cdot \eta_{\mathrm{j}_1} \cdot \eta_{\mathrm{j}_2}$ | | | | ✓ | | |
| $p_{\mathrm{T}}(\mathrm{j}_1)$ | | | | | | ✓ |
| $p_{\mathrm{T}}(\mathrm{j}_2)$ | | | | | | ✓ |
| $\Delta\phi(\mathrm{j}_1, E_{\mathrm{T}}^{\mathrm{miss}})$ | | | | ✓ | | ✓ |
| $\Delta\phi(\mathrm{j}_2, E_{\mathrm{T}}^{\mathrm{miss}})$ | | | | ✓ | | ✓ |
| $\eta$-centrality$(\ell_H)$ | | | | ✓ | | ✓ |
| $\eta$-centrality$(\ell_\tau)$ | | | | ✓ | | ✓ |

# LFV - Systematics

| 2 POI<br>Source of uncertainty | Impact on observed [$10^{-4}$]<br>$\hat{\mathcal{B}}(H \to e\tau)$ | <br>$\hat{\mathcal{B}}(H \to \mu\tau)$ |
|---|---|---|
| Flavour tagging | 0.7 | 0.2 |
| Misidentified background ($e\tau_{\text{had}}$) | 2.1 | 0.3 |
| Misidentified background ($e\tau_{\mu}$) | 2.7 | 0.3 |
| Misidentified background ($\mu\tau_{\text{had}}$) | 0.6 | 1.4 |
| Misidentified background ($\mu\tau_{e}$) | 0.9 | 1.0 |
| Jet and $E_{\text{T}}^{\text{miss}}$ | 1.2 | 0.9 |
| Electrons and muons | 1.4 | 0.5 |
| Luminosity | 0.6 | 0.4 |
| Hadronic $\tau$ decays | 0.9 | 0.9 |
| Theory (signal) | 0.8 | 0.8 |
| Theory ($Z$ + jets processes) | 0.8 | 1.0 |
| $Z \to \ell\ell$ normalisation ($e\tau$) | <0.1 | <0.1 |
| $Z \to \ell\ell$ normalisation ($\mu\tau$) | 0.2 | 0.9 |
| Background sample size | 3.7 | 2.3 |
| Total systematic uncertainty | 5.1 | 3.6 |
| Data sample size | 3.0 | 2.7 |
| Total | 5.9 | 4.5 |

Image: A. J. Gomes Delegido

# LFV - Fit Setup

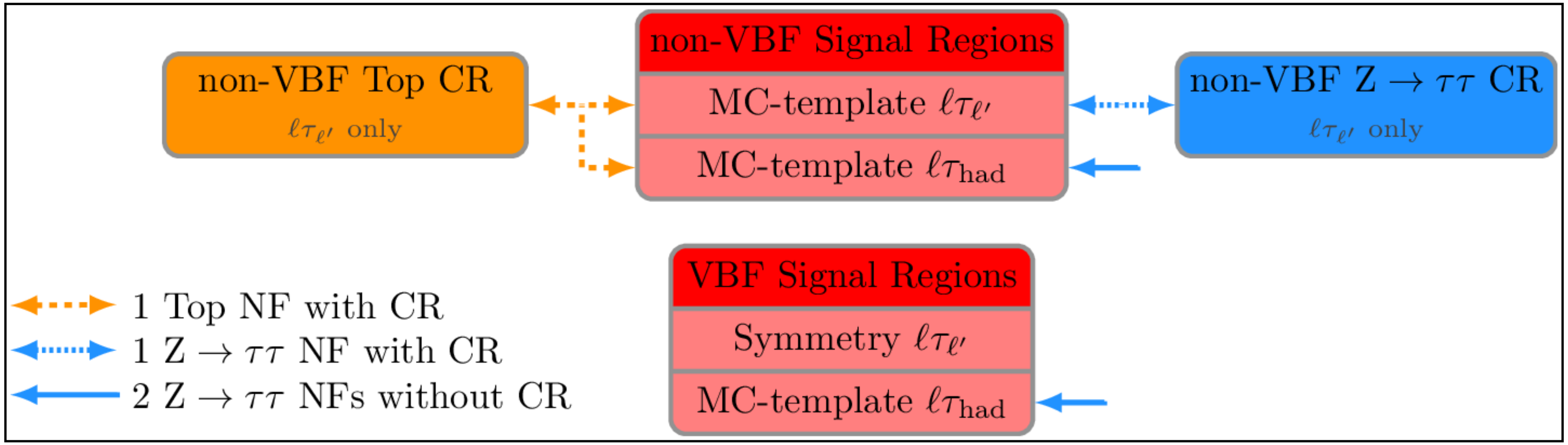


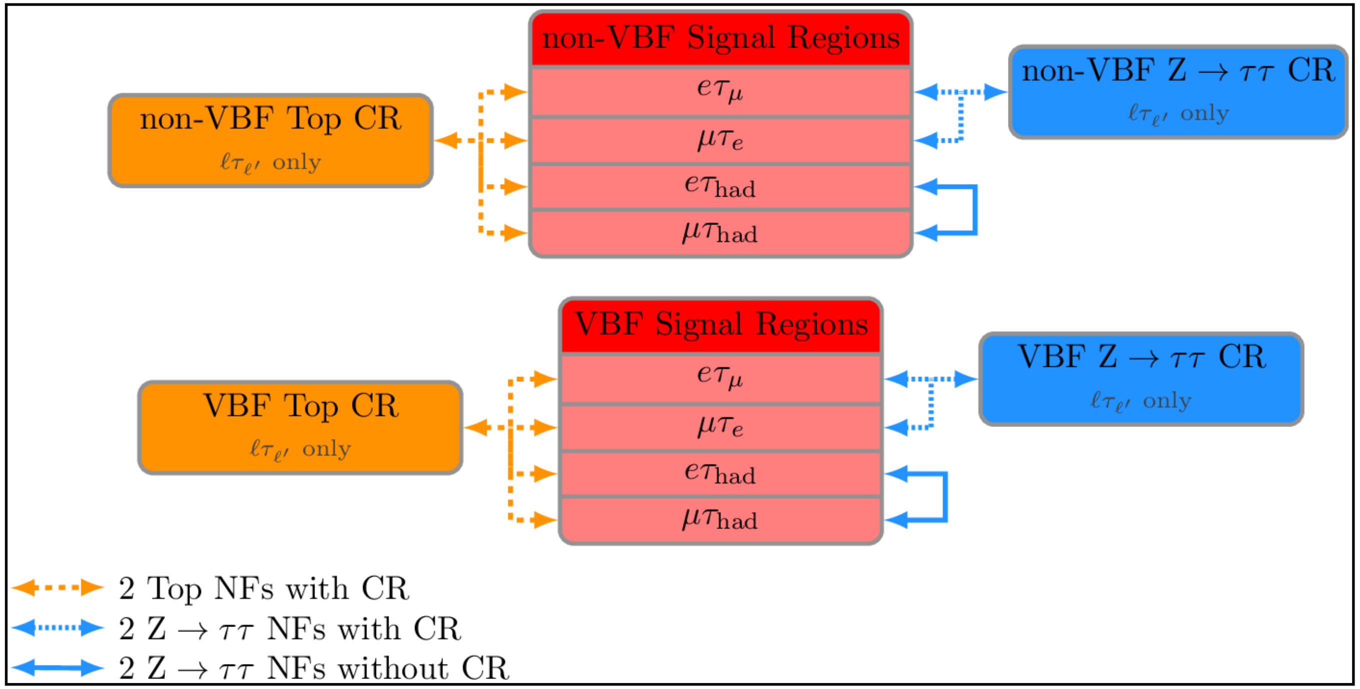

# LFV - MVAs

## Symmetry based leplep

NNs trained with Keras

Separate training for Non VBF and VBF. Shared between $e\tau_\mu$ and $\mu\tau_e$

### Non VBF

1 Multiclassifier NN with 3 output nodes. Signal output node used for fit.

### VBF

3 BDTs. Scores combined linearly.
- LFV vs. $Z\tau\tau$+$H\tau\tau$+MCfakes
- LFV vs. Top+$VV$+$HWW$
- LFV vs. Fakes

## MC-template leplep

BDTs with TMVA

Separate training for Non VBF and VBF. Shared between $e\tau_\mu$ and $\mu\tau_e$

### Non VBF and VBF

3 BDTs. Scores combined linearly.
- LFV vs. $Z\tau\tau$+$H\tau\tau$+$Z\ell\ell$
- LFV vs. Top+$VV$+$HWW$
- LFV vs. Fakes

## MC-template lephad

BDTs with TMVA

Separate trainings for Non VBF and VBF and for $e\tau_\mu$, $\mu\tau_e$

### Non VBF $e\tau$

3 BDTs. Scores combined linearly.
- LFV vs. $Z\tau\tau$
- LFV vs. Fakes
- LFV vs. Other backgrounds

### Non VBF $\mu\tau$ and VBF

2 BDTs. Scores combined linearly (NonVBF $\mu\tau$) or quadratically (VBF).
- LFV vs. $Z\tau\tau$
- LFV vs. Other backgrounds

Image: A. J. Gomes Delegido

# LFV - 1 PoI Fit

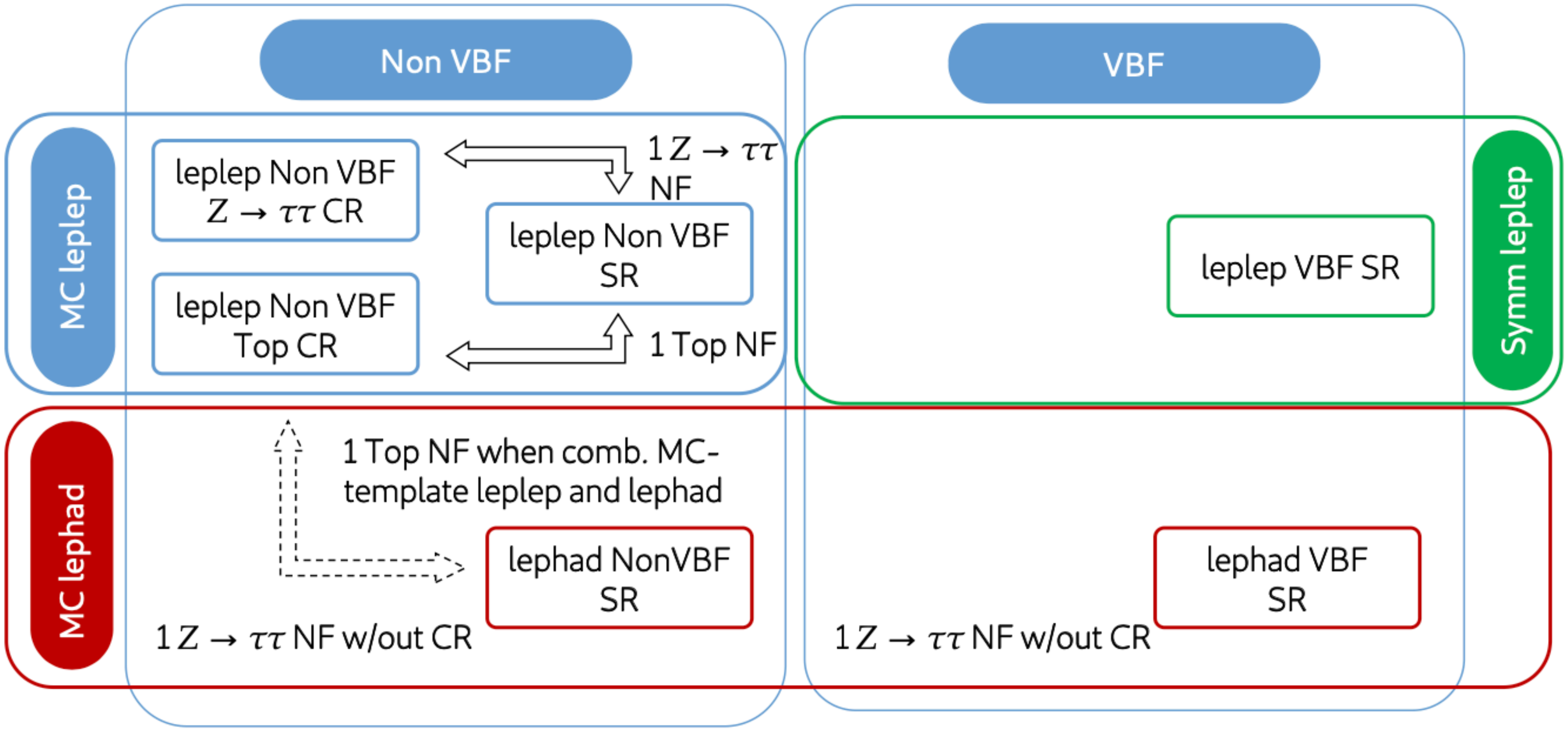


Image: A. J. Gomes Delegido

# LFV - 2 PoI Fit

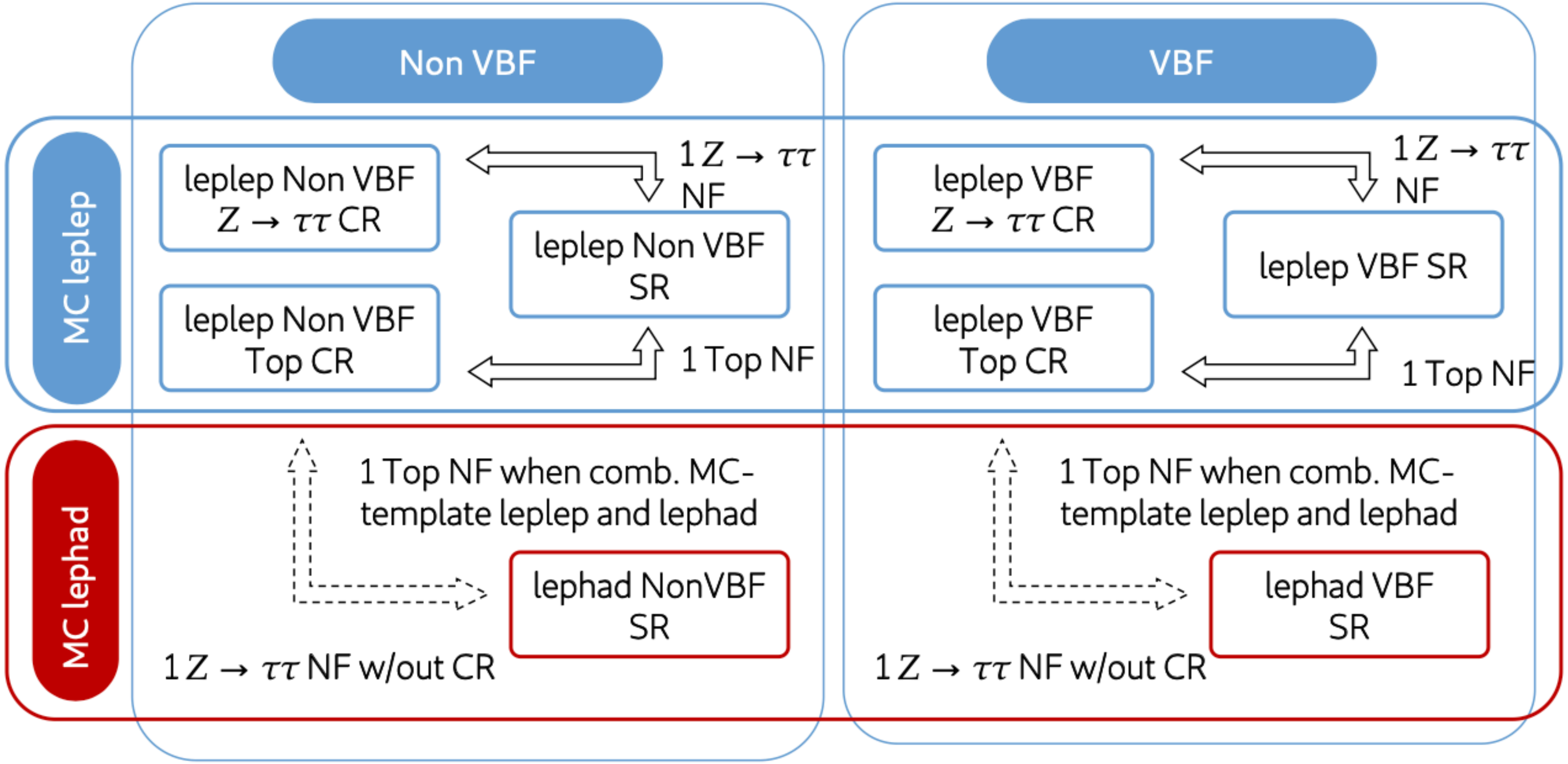


Image: A. J. Gomes Delegido

# Outlook

# LFV HL-LHC Projection - Assumptions

- **Higher CoM energy 14/13 -> 1.1**
- **Higher Integrated Lumi L(HL-LHC)/L(Run2)= 3000/140 = 21**
  - **SF Stat. unc. on MC = 0 OR alternatively SF=1/Sqrt(SF_L) = 0.21**
- **Detector updates**
- **More precise theory calculations [Eur. Phys. J. C 78 (2018) 962]**
- **Scale systematic SFs according to det. Upgrade and th precision**
- **Better object Reco (ETMISS & flavour tagging)**
- **Harsher detector conditions (<mu> = 25 (R2), 60 (R3), 140-200 (HL-LHC))**
- **1% Lumi uncertainty**
- **Thad stat. Unc. negligible**

| Uncertainties | $SF_{Syst}$ |
|---|---|
| $E_T^{miss}$ | 0.50 |
| Flavour tagging $c$- and $b$-jets | 0.50 |
| Jet, others | 1.00 |
| Electron and muon | 1.00 |
| $\tau_{had\text{-}vis}$ ID, stat.-related | 0.00 |
| $\tau_{had\text{-}vis}$, others | 1.00 |
| Data-driven estimates, stat.-related | 0.21 |
| Data-driven estimates, others | 1.00 |
| Bkg. modelling, PDF | 0.40 |
| Sig. modelling, PDF | [0.41, 0.46] |
| Modelling, others | 0.50 |
| Luminosity | 0.59 |

MC Template method fit setup projection (syst dominant in both scenarios)

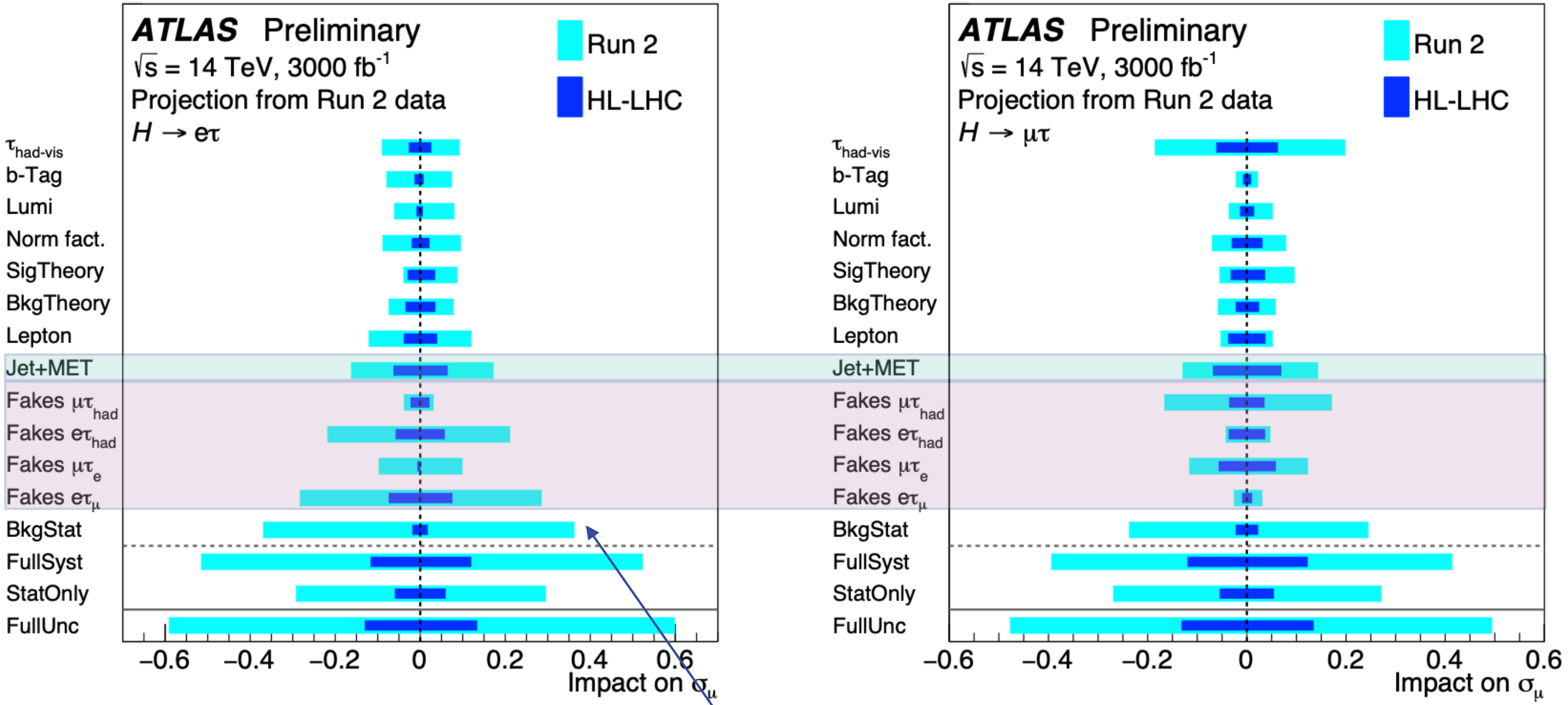


Jet+MET and fakes dominant

Stat. Unc. On bkg prediction reduced

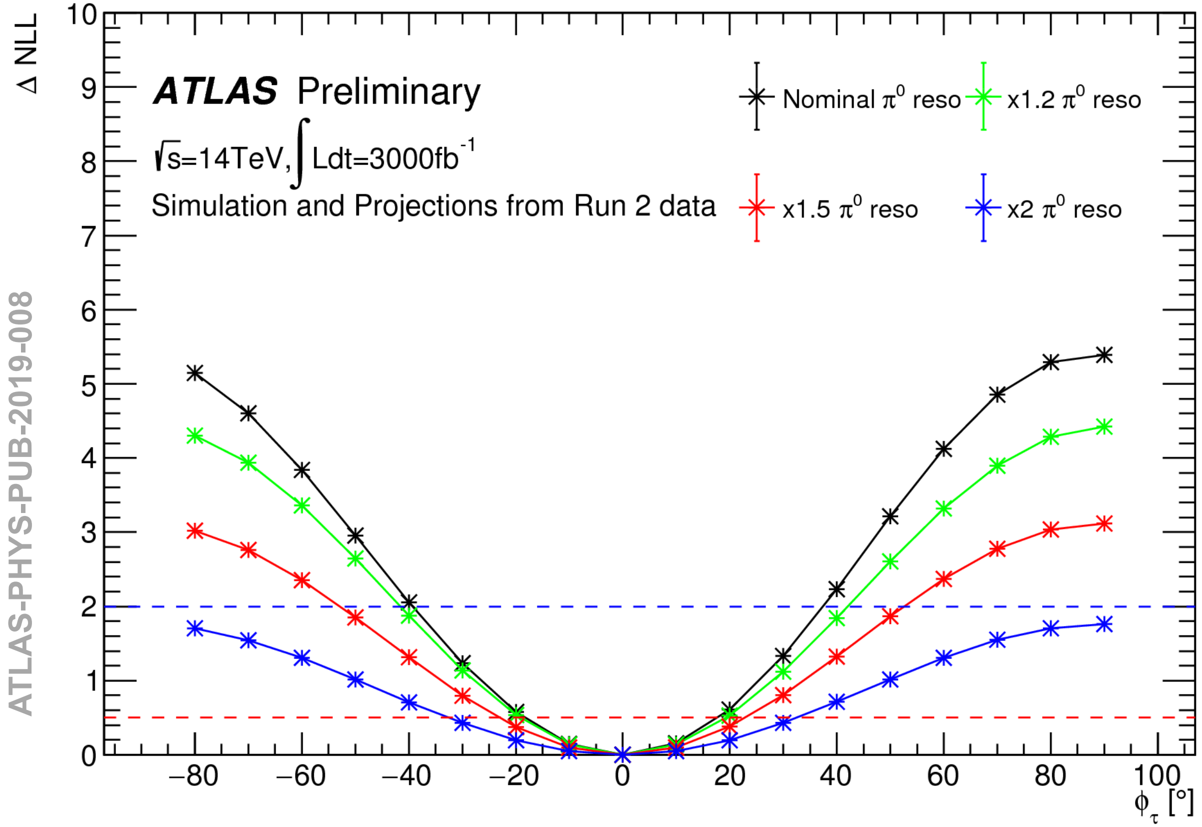


Expected uncertainty on the angle reduces to $\pm 18^{\circ}$ compared to $\pm 28^{\circ}$ in run 2 analysis

# DeepSets Decay Mode Classification for Run 3

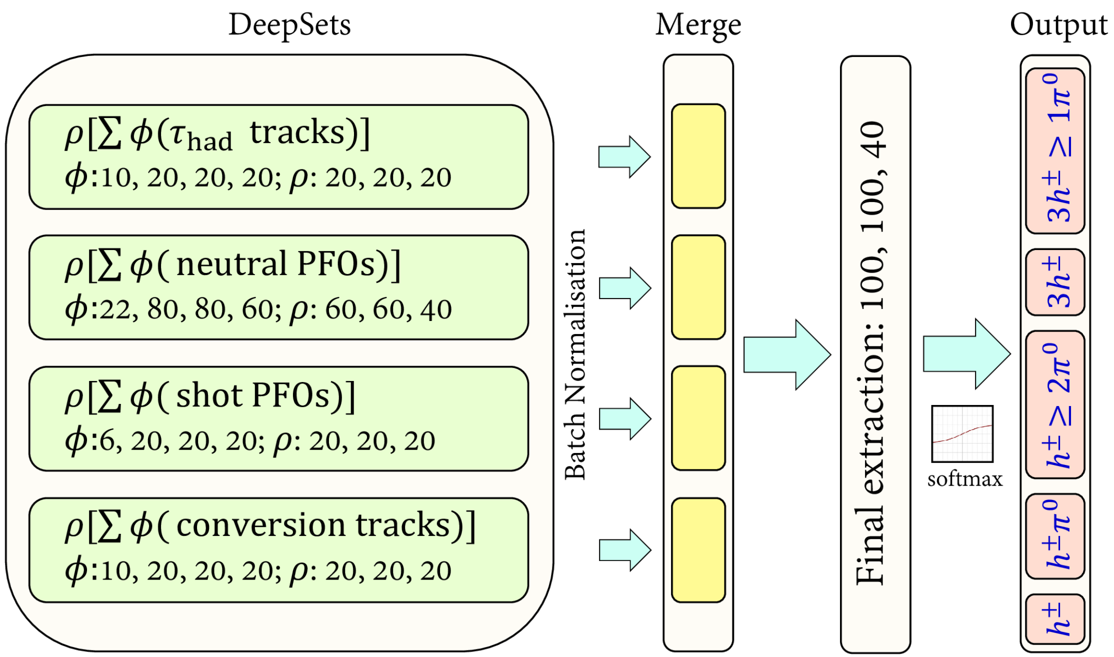


Training Parameters

| Parameter | Value |
|---|---|
| Epochs | 100* |
| Batch size | 1000 |
| Optimizer | *Adam* |
| Learning rate | 0.01* |
| $\beta_1$, $\beta_2$ | 0.9, 0.999 |
| Activation function | ReLU |

- The $h^{\pm}$ in $\tau_{\text{had}}$ decay, obtained from the $\tau_{\text{had-vis}}$ tracks (reconstructed $\tau_{\text{had}}$ tracks);
- The selected $\pi^0$ candidates that can come from the $\tau_{\text{had}}$ decay or $h^{\pm}$ remnants, pile-up, etc (referred to as $\pi^0$ candidates or Neutral PFOs);
- The local energy maxima in the EM1 layer of EM calorimeter associated with a photon from the $\pi^0$ candidate decay (referred to as photon shots or shot PFOs);
- The reconstructed conversion tracks produced by $\gamma \to e^+e^-$.

Hereafter, an 'object' refers to a $\tau_{\text{had}}$ track, $\pi^0$ candidates, photon shots or conversion track. For all

| Variable | Description |
|---|---|
| $p_T(\tau_{had})$ | $p_T$ of the $\tau_{had}$ (using calorimeter based $\tau_{had\text{-}vis}$ energy scale) |
| $p_T(\text{object})$ | $p_T$ of the object |
| $\Delta\phi(\text{object}, \tau_{had})$ | Distance between the object and $\tau_{had}$ in $\phi$ |
| $\Delta\eta(\text{object}, \tau_{had})$ | Distance between the object and $\tau_{had}$ in $\eta$ |
| $\Delta\phi(\text{object}, \text{trackECal})$ | Distance between the object and the extrapolation of highest-$p_T$ $\tau_{had}$ track to EM calorimeter in $\phi$ |
| $\Delta\eta(\text{object}, \text{trackECal})$ | Distance between the object and the extrapolation of highest-$p_T$ $\tau_{had}$ track to EM calorimeter in $\eta$ |

| Variable | Description |
|---|---|
| $\langle \eta^1 \rangle$ | First moment in $\eta$ in cluster shower axis |
| $\log(\langle r^2 \rangle)$ | Second moment in the radial distance of cluster cells from the shower axis |
| $\Delta\theta$ | Distance in $\theta$ between the EM shower axis and the vector pointing from the primary vertex to the centre of the shower |
| $\log(\lambda_{\text{centre}})$ | Distance of the cluster shower centre from the calorimeter front face measured along the shower axis |
| $\langle \lambda^2 \rangle$ | Mean distance of a cell from the shower centre along the shower axis |
| $\log(\langle \rho^2 \rangle)$ | Second moment in the cluster energy density, where $\rho = E^{\text{cluster}}/V^{\text{cluster}}$ |
| $f_{\text{core}}$ | Sum of energy fractions in the most energetic cells per sampling |
| $f_{\text{core}}^{\text{EM1}}$ | Same as $f_{\text{core}}$ but only consider EM1 |
| $N_{\text{pos,EM1}}$ | Number of cells with positive energy in EM1 |
| $N_{\text{pos,EM2}}$ | Number of cells with positive energy in EM2 |
| $E_{\text{EM1}}$ | Energy in the EM1 layer |
| $E_{\text{EM2}}$ | Energy in the EM2 layer |
| $\langle \eta^1_{\text{EM1}} \rangle$ w.r.t. cluster | First moment in $\eta$ in EM1 with respect to the cluster |
| $\langle \eta^1_{\text{EM2}} \rangle$ w.r.t. cluster | First moment in $\eta$ in EM2 with respect to the cluster |
| $\log(\langle \eta^2_{\text{EM1}} \rangle)$ w.r.t. cluster | Second moment in $\eta$ in EM1 with respect to the cluster |
| $\log(\langle \eta^2_{\text{EM2}} \rangle)$ w.r.t. cluster | Second moment in $\eta$ in EM2 with respect to the cluster |

# DeepSet improvement over BDT